



Deposited via The University of Sheffield.

White Rose Research Online URL for this paper:

<https://eprints.whiterose.ac.uk/id/eprint/152100/>

Version: Accepted Version

---

**Article:**

Frey, A.M., Satur, M.J., Phansopa, C. et al. (2019) Characterization of *Porphyromonas gingivalis* sialidase and disruption of its role in host–pathogen interactions. *Microbiology*, 165 (11). pp. 1181-1197. ISSN: 1350-0872

<https://doi.org/10.1099/mic.0.000851>

---

© The Authors 2019. The definitive peer reviewed, edited version of this article is published in *Microbiology*, 2019, <https://doi.org/10.1099/mic.0.000851>.

**Reuse**

Items deposited in White Rose Research Online are protected by copyright, with all rights reserved unless indicated otherwise. They may be downloaded and/or printed for private study, or other acts as permitted by national copyright laws. The publisher or other rights holders may allow further reproduction and re-use of the full text version. This is indicated by the licence information on the White Rose Research Online record for the item.

**Takedown**

If you consider content in White Rose Research Online to be in breach of UK law, please notify us by emailing [eprints@whiterose.ac.uk](mailto:eprints@whiterose.ac.uk) including the URL of the record and the reason for the withdrawal request.



This is a repository copy of *Characterization of Porphyromonas gingivalis sialidase and disruption of its role in host–pathogen interactions.*

White Rose Research Online URL for this paper:  
<http://eprints.whiterose.ac.uk/152100/>

Version: Submitted Version

---

**Article:**

Frey, A.M., Satur, M.J., Phansopa, C. [orcid.org/0000-0003-4943-9228](https://orcid.org/0000-0003-4943-9228) et al. (7 more authors) (2019) Characterization of Porphyromonas gingivalis sialidase and disruption of its role in host–pathogen interactions. Microbiology. ISSN 1350-0872

<https://doi.org/10.1099/mic.0.000851>

---

**Reuse**

Items deposited in White Rose Research Online are protected by copyright, with all rights reserved unless indicated otherwise. They may be downloaded and/or printed for private study, or other acts as permitted by national copyright laws. The publisher or other rights holders may allow further reproduction and re-use of the full text version. This is indicated by the licence information on the White Rose Research Online record for the item.

**Takedown**

If you consider content in White Rose Research Online to be in breach of UK law, please notify us by emailing [eprints@whiterose.ac.uk](mailto:eprints@whiterose.ac.uk) including the URL of the record and the reason for the withdrawal request.



[eprints@whiterose.ac.uk](mailto:eprints@whiterose.ac.uk)  
<https://eprints.whiterose.ac.uk/>

1

# 2 Characterisation of *Porphyromonas gingivalis* sialidase 3 and disruption of its role in host-pathogen interactions

4 Andrew M Frey<sup>1,2\*</sup>, Marianne Satur<sup>1</sup>, Chatchawal Phansopa<sup>1</sup>, Kiyonobu Honma<sup>3</sup>, Paulina A  
5 Urbanowicz<sup>5</sup>, Daniel Spencer<sup>5</sup>, Jonathan Pratten<sup>4</sup>, David Bradshaw<sup>4</sup>, Ashu Sharma<sup>3\*</sup> & Graham P  
6 Stafford<sup>1\*</sup>

## 7 Affiliations

8 <sup>1</sup> Integrated BioSciences, School of Clinical Dentistry, The University of Sheffield, 19 Claremont  
9 Crescent, Sheffield S10 2TA, U.K.

10 <sup>2</sup> University of South Florida, Department of Cell Biology, Microbiology, and Molecular Biology, 4202  
11 East Fowler Ave, ISA2015, Tampa, FL 33620

12 <sup>3</sup> Dept. of Oral Biology, University at Buffalo, Buffalo, NY, United States.

13 <sup>4</sup> Oral Health R&D, GlaxoSmithKline, St. Georges Avenue, Weybridge, KT13 0DE, U.K.

14 <sup>5</sup> Ludger Ltd., Culham Science Centre, Oxfordshire, OX14 3EB, U.K.

15 \* Corresponding authors

16 Graham Stafford- [g.stafford@sheffield.ac.uk](mailto:g.stafford@sheffield.ac.uk), phone: 0044 (114) 2159413

17 Ashu Sharma- [sharmaa@buffalo.edu](mailto:sharmaa@buffalo.edu), phone: 001 (716) 8292759

18 Andrew Frey- [andrewfrey@usf.edu](mailto:andrewfrey@usf.edu), 001 (813) 9745259

19 **Keywords:** Sialidase, host-pathogen interactions, biofilm, glycoprotein, periodontitis, gingivitis

## 20 Abstract

21 Key to onset and progression of periodontitis is a complex relationship between oral bacteria and  
22 the host. The organisms most associated with severe periodontitis are the periodontal pathogens of  
23 the red complex; *Tannerella forsythia*, *Treponema denticola*, and *Porphyromonas gingivalis*. These  
24 organisms express sialidases, which cleave sialic acid from host glycoproteins, and contribute to  
25 disease through various mechanisms. Here, we expressed and purified recombinant *P. gingivalis*  
26 sialidase SiaPG (PG\_0352) and characterised its activity on a number of substrates, including host  
27 sialoglycoproteins and highlighting inability to cleave diacetylated sialic acids a phenomenon  
28 overcome by the NanS sialate-esterase from *T. forsythia*. Indeed SiaPG required NanS to maximise  
29 sialic acid harvesting from heavily O-acetylated substrates such as bovine salivary mucin, hinting at  
30 the possibility of interspecies cooperation in sialic acid release from host sources by these members  
31 of the oral microbiota. Activity of SiaPG and *P. gingivalis* was inhibited using the commercially  
32 available chemotherapeutic zanamivir, indicating its potential as a virulence inhibitor, which also  
33 inhibited sialic acid release from mucin, and was capable of inhibiting biofilm formation of *P.*  
34 *gingivalis* on oral glycoprotein sources. Zanamivir also inhibited attachment and invasion of oral

35 epithelial cells by *P. gingivalis* and other periodontal pathogens, both in monospecies but also in  
36 multispecies infection experiments, indicating potential to suppress host-pathogen interactions of a  
37 mixed microbial community. This study broadens our understanding of the multifarious roles of  
38 bacterial sialidases in virulence, and indicates that their inhibition with chemotherapeutics could be  
39 a promising strategy for periodontitis therapy.

## 40 Introduction

41 The black-pigmented, Gram negative, asaccharolytic anaerobe *Porphyromonas gingivalis* has been  
42 the focus of much research due to its role in periodontitis where it is often referred to as a  
43 “keystone pathogen” [1]. *P. gingivalis* exists as a small part of the microbiome, which sees a  
44 population shift to include a greater proportion of certain bacterial species, a state now referred to  
45 as dysbiosis [2]. In periodontal disease this population shift was observed in the 1990’s, with certain  
46 organisms considered particularly important to periodontal disease. *Tannerella forsythia*,  
47 *Porphyromonas gingivalis*, and *Treponema denticola* form the so-called red complex which is  
48 strongly associated with disease [3], and with the advent of next generation sequencing their  
49 presence as a signature of periodontal disease has been well established, along with other  
50 organisms which seem to play a causative role in periodontitis [2, 4]. During treatment of  
51 periodontitis systemic antibiotics such as azithromycin can be administered as an adjunct to  
52 mechanical removal of the subgingival plaque [5]. Despite this a proportion of patients poorly  
53 respond to periodontal therapy, and in these patients (post-treatment) the levels of periodontal  
54 pathogens are higher than in patients who respond to treatment, or in healthy controls [6]. This  
55 difficulty in treatment has led to increased interest in development of an “anti-virulence approach”  
56 to target the virulence factors of specific pathogens or groups of pathogens, including those  
57 responsible for periodontitis. This has been seen in the case of the gingipains of *P. gingivalis*, with  
58 several plant extracts [7, 8], and short peptides [9] shown to reduce gingipain activity, with *in vitro*  
59 studies showing reductions in *P. gingivalis* biofilm formation [8], and disruption of bacterial nutrient  
60 acquisition leading to decreased *P. gingivalis* growth [9]. Plant extracts that inhibit gingipains have  
61 also shown disruption of host-*P. gingivalis* interactions; attachment and invasion of host cells, and  
62 cytokine production [7]. Moreover, a recent study showed that treatment with a potent small  
63 molecule gingipain inhibitor in mice reduced *P. gingivalis* infection in the brain and further blocked  
64 A $\beta$ <sub>1-42</sub> production and neurodegenerative Alzheimer disease pathology [10].

65 Another virulence factor of periodontal pathogens including *P. gingivalis* are sialidases (also called  
66 neuraminidases), enzymes frequently expressed by host-dwelling organisms which cleave terminal  
67 sialic acid—a family of 9-carbon sugars—from host sialoglycans. In humans the most common sialic acid  
68 is N-acetylneuraminic acid (Neu5Ac), and is usually linked by its second carbon to the third or sixth  
69 carbon of the underlying sugar ( $\alpha$ 2-3 or  $\alpha$ 2-6 linked sialic acid). Sialidases are well established  
70 virulence factors in the gut and nasopharyngeal pathogens *Vibrio cholerae* and *Streptococcus*  
71 *pneumoniae*, where they contribute to colonisation, persistence, and ultimately disease [11, 12].  
72 Interestingly, all three periodontal red complex pathogens express a sialidase; PG\_0352 (termed  
73 SiaPG here) in *P. gingivalis*, NanH in *T. forsythia*, and TDE0471 in *T. denticola*. Other periodontal

74 pathogens also possess mechanisms to process sialic acid in the absence of sialidase expression,  
75 such as some *Fusobacterium nucleatum* spp., which possess neuraminidase for catabolism of  
76 sialic acid [13]. It is thought that acquisition of sialic acid by organisms that do not possess sialidases  
77 is due to the overall action of the microbial community of which they are part of. Additionally,  
78 periodontal organisms tentatively associated with health such as *Veillonella* spp. [14] and the  
79 recently characterised *Tannerella* HOT (oral taxon BU063) [15] do not possess sialidases. The  
80 apparent importance of sialidases for periodontal pathogens has been investigated in studies of  
81 sialidase knockout. *T. forsythia nanH* sialidase mutants displayed decreased attachment to oral  
82 epithelial cells compared to their parent strain [16]. Different strains of *P. gingivalis* have also been  
83 made deficient in SiaPG [17, 18], although the exact implications for virulence are less clear because  
84 the sialidase mutants display defects in capsule formation. Mutant strains do show decreased  
85 association with host cells, while the virulence of  $\Delta$ *siaPG* mutants in a mouse abscess model is also  
86 decreased relative to the parent strain, where subcutaneous injections of wild type *P. gingivalis*  
87 (strain W83) resulted in the formation of abscesses and ultimately lethal infection that were not  
88 seen in sialidase deficient *P. gingivalis* [17]. Sialidase deficient mutants of *T. denticola* have also been  
89 studied, and these display reduced complement evasion and decreased virulence in a mouse abscess  
90 model [19].

91 Given the importance of sialidases for periodontal pathogen-host interactions and subsequent  
92 virulence, abrogation of sialidase activity using sialidase inhibitors might exert anti-virulence effects  
93 or be detrimental to the lifecycle of these organisms. This is particularly pertinent given recent  
94 evidence that levels of sialidase transcript (*T. forsythia nanH* gene) are elevated in periodontal  
95 disease [20]. Similarly, sialidase enzyme activity is raised in the gingival crevicular fluid of patients  
96 with periodontal disease and this high sialidase activity is an indicator of poor responsiveness to  
97 standard treatment [21].

98 Sialidase inhibitors are undergoing extensive development and some are available as a treatment for  
99 influenza, with the sialidase inhibitors oseltamivir and zanamivir licensed for use globally. Sialidase  
100 inhibition has been investigated in *T. forsythia*, where the inhibitor oseltamivir was shown to disrupt  
101 biofilm formation on host sialoglycan substrates [16]. Considering the above, we set out to further  
102 characterise the sialidase of *P. gingivalis*, performing a biochemical characterisation and  
103 establishing an activity profile while also examining the potential of sialidase inhibitors to modulate  
104 pathogenesis of *P. gingivalis* alone and in combination with a range of other periodontal pathogens  
105 with the commercially available sialidase inhibitor zanamivir.

## 106 **Methods**

107 **Bacterial strains, human cell lines, and culture conditions** *Tannerella forsythia* strains used here  
108 were the WT type strain ATCC 43037, supplied by William Wade, Queen Mary University of London,  
109 UK, and the sialidase deficient *nanH* mutant (TF $\Delta$ nanH) [22]. *Porphyromonas gingivalis* strains used  
110 here were the WT strains ATCC 33277, 381 (Pg381), and a sialidase deficient mutant of Pg381  
111 (Pg381 $\Delta$ SiaPG). *Fusobacterium nucleatum* strain NCTC 25586 (subspecies nucleatum) was also used  
112 in this study, supplied by William Wade. All strains were cultured at 37 °C under anaerobic  
113 conditions (10 % CO<sub>2</sub>, 10 % H<sub>2</sub>, 80 % N<sub>2</sub>) in a Don-Whitley mini-macs anaerobic cabinet. *P. gingivalis*  
114 and *F. nucleatum* strains were cultured on Fastidious Anaerobe Agar (Lab M, Lancashire, UK)  
115 supplemented with 5 % (v/v) oxalated horse blood (Thermo Fisher Scientific, UK), for 2-3 days before  
116 harvesting for use in experiments. *T. forsythia* strains were cultured on Fastidious Anaerobe Agar  
117 (Lab M, UK) supplemented with 5 % (v/v) oxalated Horse Blood (Thermo Fisher Scientific), 10  $\mu$ g ml<sup>-1</sup>  
118 N-acetylneuraminic acid (NAM, Sigma Aldrich, UK), and 25  $\mu$ g ml<sup>-1</sup> Gentamicin (Sigma-Aldrich) for 3-7  
119 days before harvesting for use in experiments. In addition, TF $\Delta$ nanH and Pg381 $\Delta$ SiaPG were  
120 intermittently subcultured in the presence of 10  $\mu$ g ml<sup>-1</sup> erythromycin to ensure maintenance of the  
121 antibiotic resistance cassette marker responsible for sialidase inactivation. Immortalized human oral  
122 keratinocytes (OKF6/Tert2) (Dickson et al. 2000) were kindly provided by Dr J. Rheinwald (Harvard  
123 Medical School, Cambridge, MA) and were grown in keratinocyte-serum free media supplemented  
124 with defined growth supplements (DKSFM, Fisher Scientific, Loughborough, UK). The Oral Squamous  
125 Cell Carcinoma (OSCC) cell line H357 (Thomas et al. 2001; Sugiyama et al. 1993)-a generous gift from  
126 Professor S. Prime, University of Bristol, UK-was grown in Dulbecco's Modified Eagle Medium  
127 (DMEM) supplemented with 10 % (v/v) foetal bovine serum (FBS), 2mM L-glutamine, and 100 units  
128 ml<sup>-1</sup> Penicillin-Streptomycin (Sigma Aldrich). Cells were incubated at 37 °C, 5 % CO<sub>2</sub> when not  
129 undergoing media changes or passaging. Cells were grown to 70–90 % confluence and media was  
130 changed every 2–4 days. OBA-9 cells were maintained in keratinocyte basal medium KGM-2  
131 supplemented with epidermal growth factor (EGF), bovine pituitary extract, epinephrine, transferrin,  
132 hydrocortisone and insulin, as per the manufacturer's recommendations (Lonza). Cells were used  
133 after reaching near confluence.

134 **Cloning, expression, and purification of recombinant proteins** NanH and NanS were cloned,  
135 expressed, and purified as previously described [23, 24]. A nucleotide sequence encoding SiaPG  
136 (PG\_0352, based on the genome of strain ATCC 33277) without the secretion signal sequence  
137 (supplemental text), was codon optimised for expression in *E. coli*, and synthesized commercially  
138 (ThermoFisher). The sequence also contained restriction sites for *NdeI* and *XhoI* at its 5' and 3' ends,  
139 enabling it to be ligated into pET vectors. Restriction digest and ligation was performed using NEB  
140 buffers, restriction enzymes, and T4 ligase, according to manufacturer's protocols. SiaPG was ligated

141 into pET21a, and ultimately transformed into chemically competent *E. coli* BL21 (origami B).  
142 Expression and purification of recombinant SiaPG was performed as previously described for NanH  
143 [24].

#### 144 **Construction of *P. gingivalis* *siaPG* deletion mutant and genetic complementation.**

145 For generating a sialidase deficient mutant, the *siaPG* gene (PG0352) in *P. gingivalis* 381 strain was  
146 inactivated by an allelic replacement strategy. The primers used in the construction and  
147 complementation strategy are listed in Table 1. Briefly, a DNA fragment containing PG0352 coding  
148 region and flanking sequences was PCR amplified with Primers #1 and #2 using the *P. gingivalis* 381  
149 gDNA. This product was then used as a template to amplify the upstream and downstream regions  
150 of PG0352 with primer sets #1 and #3 (for '5 end) and #2 and #5 (for '3 end), respectively. In parallel,  
151 the *ermF* gene (797 bp) was amplified from the plasmid pVA2198 with Primers #4 and #6. Primers  
152 #3, #4, #5, and #6 contain overlapping sequences for *ermF* and PG0352 to allow generation of a  
153 fusion fragment via overlap PCR. Finally, PCR products of PG0352 with flanking regions and *ermF*  
154 gene were combined in an overlap PCR reaction using primers #1 and #2. The overlap PCR product  
155 was sequenced to confirm the correct fusion of fragments and then transformed into *P. gingivalis*  
156 381 by electroporation as previously described [25]. Transformants were plated on TSB-blood agar  
157 plates containing 10 µg ml<sup>-1</sup> of erythromycin and incubated at 37 °C anaerobically for 10 days.  
158 Following incubation, erythromycin-resistant colonies were screened by PCR and Southern blotting.  
159 One representative deletion mutant as confirmed by PCR and Southern blotting (data not shown)  
160 and showing no sialidase activity was selected and designated as Pg381Δ*siaPG*. For  
161 complementation of Pg381Δ*siaPG*, in trans complementation with the *siaPG* gene on the self-  
162 replicating shuttle plasmid pT-COW was employed as we have performed previously [25]. Briefly, the  
163 *siaPG* gene fragment amplified by PCR with the primers FWD *Bam*HI and REV *Sal*II (Table 1) was  
164 digested with *Bam*HI and *Sal*II and ligated into *Bam*HI and *Sal*II digested pT-COW plasmid. The resulting  
165 plasmid, pT-PG352C was transformation into Pg381Δ*siaPG* by tri-parental conjugation involving with  
166 Pg381Δ*siaPG*, *E. coli* carrying shuttle vector pT-PG352C and *E. coli* carrying helper plasmid pRK231  
167 4,5. The transformants were selected on TSB-blood agar plate containing 100 µg ml<sup>-1</sup> of gentamicin  
168 (Invitrogen), 10 µg ml<sup>-1</sup> of erythromycin (Sigma) and 1 µg ml<sup>-1</sup> of tetracycline (Sigma). The completed  
169 clones with sialidase expression were saved and one random clone designated Δ*siaPG*<sup>+</sup> served as a  
170 representative.

171 **Inhibition of whole periodontal pathogens and purified sialidases by zanamivir.** Zanamivir was  
172 provided by GlaxoSmithKline (GSK, Weybridge, UK). Whole *T. forsythia* or *P. gingivalis*, or purified  
173 sialidases 2.5 nM NanH or 5 nM rSiaPG were incubated in the presence of 0.1 mM MUNANA, in 50

174 mM Sodium Phosphate 200 mM NaCl, pH 7.4 (to mimic host physiological conditions), in the  
175 presence of different concentrations of zanamivir (0-10 mM). Sialidase inhibition was expressed as  
176 the percentage change in fluorescence at a given concentration of inhibitor, relative to fluorescence  
177 in the absence of inhibitor. Sialidase inhibition (%) was plotted against log[inhibitor], and the  
178 variable slope model applied to obtain the IC<sub>50</sub> of zanamivir for SiaPG and NanH in Graphpad Prism  
179 7, using the equation:  $Y=100/(1+10^{(\text{LogIC}_{50}-X) \times \text{Hillslope}})$ . Y = sialidase activity relative to no  
180 inhibitor condition (%), X = log[inhibitor], and Hillslope = steepness of the curve.

181 **Biochemistry of SiaPG: Determination of optimum pH, reaction kinetics with MUNANA and**  
182 **sialyllactose, and sialic acid release from mucin in concert with NanS from *T. forsythia*.** Whole *P.*  
183 *gingivalis* and purified SiaPG were tested for pH optima in a similar manner to *T. forsythia* and its  
184 sialidase [24]. For whole cell assays, bacteria were resuspended from agar plates, washed 3x in  
185 phosphate buffer saline, pH 7.4 (PBS, Sigma Aldrich) and centrifugation at 10000 *g* for 2 minutes,  
186 and resuspended to an OD<sub>600</sub> of 0.05 in appropriate reaction buffers (20 mM sodium citrate–citric  
187 acid (pH 3.0–6.4), sodium phosphate mono-basic/dibasic (pH 6.8–8.8) or sodium carbonate–sodium  
188 bicarbonate (pH 9.2–10.5)). For pH optimum derivation for purified SiaPG, enzyme was used at 2.5  
189 nM. In both cases, cells or enzyme were incubated with 100 μM Mu-NANA and quenched with  
190 addition of 100 mM sodium carbonate buffer, pH 10.5, at a volume ratio of 1 : 1.5 (reaction: sodium  
191 carbonate), and sialidase activity quantified by measuring 4-MU fluorescence ( $\lambda_{\text{exc}} = 350 \text{ nm}$ ;  $\lambda_{\text{em}} =$   
192  $450 \text{ nm}$ ). For whole *P. gingivalis* assays were performed over 1-3 hours at 37 °C, incubation with  
193 SiaPG was performed over 1-3 minutes at room temperature (~20 °C).

194 For derivation of Michaelis-Menten kinetics for SiaPG, 2.5 nM enzyme was incubated with varying  
195 concentrations of MU-NANA and again quenched. A standard curve of the fluorescence signal of 4-  
196 MU at defined concentrations was also obtained, enabling sialidase activity to be expressed as 4-MU  
197 released  $\mu\text{mol min}^{-1} \text{ mg}^{-1}$  SiaPG. Similar conditions were used for derivation of kinetic parameters  
198 with 3/6-siallyl-lactose, except no quenching was required and the levels of released sialic acid using  
199 a modified Thiobarbituric acid (TBA) assay. In this case reactions were stopped at time points over  
200 1-5 minutes by commencement of the TBA assay: Fifty microlitres of these reactions were added to  
201 25 μl of 25 mM sodium periodate (Sigma–Aldrich) in 60 mM H<sub>2</sub>SO<sub>4</sub> (Thermo Fisher) and incubated  
202 for 30 min at 37 °C. This oxidation step was stopped by the addition of 20 μl of 2% (w/v) sodium  
203 meta-arsenite (Sigma–Aldrich) in 500 mM HCl. Forty-seven microlitres of this reaction were added to  
204 100 μl of 100 mM TBA, pH 9.0, and incubated at 95 °C for 7.5 min, resulting in the thiol-labelling of  
205 free sialic acid. Upon centrifugation at 1500 G for 5 min, the pink chromophore in the clarified  
206 supernatant was spectrophotometrically quantified at A<sub>549</sub>. A standard curve of known sialic acid

207 (Neu5Ac, Carbosynth) concentrations was used to calculate sialic acid release in  $\mu\text{molmin}^{-1}\text{mg}^{-1}$   
208 SiaPG. Finally, release of Neu5Ac from mucin was assessed using BSM and the TBA assay. PBS + 6  $\mu\text{M}$   
209 BSM was incubated with combinations of 100 nM rSiaPG, 0.5 mM zanamivir, and/or the sialate-O-  
210 acetylerase NanS from *T. forsythia* (100 nM), and incubated for 30 minutes at 37 °C, before the  
211 reaction was stopped and the TBA assay commenced as described above.

212

213 **Analysis of Procainamide labelled glycans.** SLeX and FA2G2S2 (A2F) glycans (Ludger Ltd.) underwent  
214 procainamide labelling (see below), as were glycans released from recombinant human EPO as  
215 previously described [23]. Briefly, human EPO was expressed in Chinese hamster ovary (CHO) cells (a  
216 gift from Antonio Vallin, Center for Molecular Immunology, La Habana, Cuba) and released using  
217 peptide N-glycosidase F (PNGase F, E-PNG01; Ludger Ltd). EPO (in 17.5  $\mu\text{l}$ ) was denatured at 100 °C  
218 for 5 mins with the addition of 6.25  $\mu\text{l}$  2 % (w/v) SDS, and 1 M 2-mercaptoethanol, then incubated at  
219 37 °C for 16 h with 1  $\mu\text{l}$  PNGase F and 1.25  $\mu\text{l}$  15 % (w/v) Triton X-100. Released N-glycans were  
220 fluorescently labelled with 2-aminobenzamide (2-AB) as described previously [26] using a LT-KPROC-  
221 96 kit (Ludger Ltd.). The released glycans were incubated with labelling reagents for 3 h at 65 °C. The  
222 2-AB- labelled glycans were cleaned up using LudgerClean S Cartridges (Ludger Ltd), then incubated  
223 with 1  $\mu\text{l}$  of 1 mg  $\text{ml}^{-1}$  SiaPG in a final volume of 10  $\mu\text{l}$  (50 mM sodium acetate buffer, pH 5.5) for 16 h  
224 at 37 °C. Glycans were cleaned-up and SiaPG removed using a LC-PROC-96 kit (Ludger Ltd.)  
225 Procainamide labelled glycans (Ludger) were analysed by UHPLC-MS/MS. Here, 25  $\mu\text{l}$  of each sample  
226 was injected into a Waters ACQUITY UPLC Glycan BEH Amide column (2.1 x 150 mm, 1.7  $\mu\text{m}$  particle  
227 size, 130 Å pore size) at 40°C on a Dionex Ultimate 3000 UHPLC instrument with a fluorescence  
228 detector ( $\lambda_{\text{ex}}$  = 310 nm,  $\lambda_{\text{em}}$  = 370 nm) attached to a Bruker Amazon Speed ETD. Mobile phase A  
229 was a 50 mM ammonium formate solution (pH 4.4) and mobile phase B was neat acetonitrile.  
230 Analyte separation was accomplished by a gradient running from 76-51% mobile phase B over 70  
231 minutes at a flow rate of 0.4  $\text{ml min}^{-1}$ . The Amazon Speed was operated in the positive sensitivity  
232 mode using following settings: source temperature, 180 C; gas flow, 4  $\text{L min}^{-1}$ ; capillary voltage, 4500  
233 V; ICC target, 200,000; maximum accumulation time, 50.00 ms; rolling average, 2; number of  
234 precursor ions selected, 3; scan mode, enhanced resolution; mass range scanned, 400 to 1700. Data  
235 was analysed using Bruker Compass Data Analysis software v4.1 and glycan diagrams made using  
236 GlycoWorkbench v2.0. Glycan compositions were elucidated based on MS2 fragmentation.

237 **Lectin staining for cell surface sialic acid- immunofluorescence microscopy.** H357 cells were seeded  
238 at a density of  $1.5 \times 10^5$  cells  $\text{ml}^{-1}$  into the wells of a 24-well tissue culture plate which contained  
239 sterile glass coverslips (BDH). These were incubated at 37 °C, 5 %  $\text{CO}_2$  for 18 hours. Treatment with

240 SiaPG and NanH was performed by washing 2 x with PBS, then incubated with 200 nM of each  
241 sialidase for 30 minutes at 37 °C. Cells then underwent sialic acid staining with lectins from  
242 *Sambucus nigra* (FITC conjugated SNA, Vector Labs, specific for  $\alpha$ 2-6 Neu5Ac linkages), *Maackia*  
243 *amuriensis* (Biotinylated MAA, Vector Labs, specific for  $\alpha$ 2-3 Neu5Ac linkages). After treatment, cells  
244 were washed twice with 500  $\mu$ l PBS followed by application of lectins: 4  $\mu$ g ml<sup>-1</sup> SNA or 8  $\mu$ g ml<sup>-1</sup>  
245 MAA, for 30 minutes at 37 °C, 5 % CO<sub>2</sub>. Cells were washed twice with 500  $\mu$ l PBS, and conditions  
246 containing MAA underwent a second incubation with 2  $\mu$ g ml<sup>-1</sup> Texas Red-Streptavidin, for 30  
247 minutes at 37 °C. Stained cells were washed three times with 500  $\mu$ l PBS and fixed with 500  $\mu$ l 2 %  
248 (w/v) paraformaldehyde for 15 minutes at 37 °C. Coverslips with fixed cells were removed from wells  
249 and mounted onto glass slides with ProLong Gold Antifade mount (containing DAPI, ThermoFisher  
250 Scientific). Mounted cells were incubated for at least 18 hours and visualised within one week.  
251 Imaging was performed with an Axiovert 200M fluorescence microscope (Zeiss) and associated  
252 Axiovert software (Zeiss). Images were processed using Fiji-imageJ, Software [27]. Fluorescence  
253 background subtraction was performed for all images using the same parameters for each  
254 fluorescence colour channel in a given experiment.

255 **Biofilm assays.** *P. gingivalis* was cultured in the wells of a 96-well tissue culture plate (poly-lysine  
256 coated, Greiner): Bacteria from an agar plate were resuspended to an OD<sub>600</sub> of 0.05 in Tryptic Soy  
257 Broth (TSB; Sigma-Aldrich) supplemented with 2 % (w/v) yeast extract, 1  $\mu$ g ml<sup>-1</sup> vitamin K, 5  $\mu$ g ml<sup>-1</sup>  
258 hemin, 50  $\mu$ g ml<sup>-1</sup> gentamicin, and either 6 mM Neu5Ac or no additional supplements. In conditions  
259 testing host glycoproteins, 100  $\mu$ l of 6  $\mu$ M BSM, 100 % (v/v) pooled human saliva, or fetal bovine  
260 serum (FBS) was added to plate wells and left to coat the wells by incubation at 4 °C overnight,  
261 removed, and wells washed with PBS once. In conditions testing the effect of sialidase inhibition, 10  
262 mM zanamivir was included. All media was equilibrated overnight in culture conditions, namely, 37  
263 °C under anaerobic atmosphere (10 % CO<sub>2</sub>, 10 % H<sub>2</sub>, 80 % N<sub>2</sub>). Biofilms were cultured for 5 days. To  
264 quantify planktonic or total growth, all conditions underwent OD<sub>600</sub> measurement using a Tecan  
265 Infinite M200 plate reader. Quantification was carried out by either crystal violet staining or manual  
266 counting of organisms. Crystal violet solution (0.1 % w/v) was added to each well and incubated at  
267 room temperature for 30 minutes. After incubation, crystal violet was removed and wells were  
268 gently washed 3-4 times with PBS before visualisation using light microscopy or extraction with 80:  
269 20 ethanol: acetone. For manual counting, biofilms were gently washed twice using PBS to remove  
270 planktonic cells, and vigorously resuspended in PBS and serial diluted where appropriate. Bacteria  
271 were enumerated by counting using a Helber chamber (Hawksley) under phase contrast microscopy,  
272 400 x magnification.

273 **Antibiotic protection assays** H357 or OKF6 cells were seeded into the wells of a 24-well tissue  
274 culture plate at a density of  $1.2 \times 10^5$ - $2 \times 10^5$  cells and incubated for 24-48h. Media was removed,  
275 the cells in one well were detached by trypsinisation and counted by haemocytometry, to determine  
276 the number of cells per well. Remaining cells were incubated for 1 hour in media supplemented with  
277 2 % (w/v) bovine serum albumin (BSA), then washed twice with PBS. Bacteria were quantified using  
278 a Helber chamber (Hawksley) under phase contrast microscopy, 400 x magnification. Bacterial  
279 suspensions were diluted in culture media (with no FBS or antibiotics) to a ratio of 1:100 host cells:  
280 bacteria, and for inhibitor testing conditions 10 mM zanamivir was included. These suspensions were  
281 incubated with the host cells at 37 °C, 5 % CO<sub>2</sub> for 1.5 hours, or in empty wells containing no host  
282 cells-constituting a bacterial “viability” control. After incubation, the wells were washed twice with  
283 PBS, and either harvested (see below)-forming the “total association” condition, or media with 200  
284  $\mu\text{g ml}^{-1}$  metronidazole was added, then incubated at 37 °C, 5 % CO<sub>2</sub> for 1 hour, forming the  
285 “invasion” conditions. To harvest bacteria, wells were washed three times with PBS, lysed with  
286 deionised water and scraped with a pipette tip for one minute. Sufficient lysis was checked by  
287 microscopy (this method reliably resulted in >99 % lysis). Harvested bacterial suspensions  
288 underwent serial dilutions and were plated onto agar by Miles-Misra methodology. After incubation  
289 and colony counting, the number of bacteria associated with host cells was determined and  
290 expressed as a percentage of viable bacteria that were associated with and had invaded the OKF6  
291 cells. By subtracting invaded organisms from associated, the number of “attached” bacteria was  
292 obtained.

293 **Assessment of zanamivir cytotoxicity** Quantifying metabolism as an indicator of cell viability was  
294 performed using 3-(4,5-Dimethylthiazol-2-yl)-2,5-Diphenyltetrazolium Bromide (MTT). Twenty five  
295 thousand OKF6 cells in DKFSM were seeded into the wells of a 96 well tissue culture plate (Greiner),  
296 and incubated for 24 hours at 37 °C, 5 % CO<sub>2</sub>. Cells were then washed twice with PBS, and media  
297 supplemented with 1 mg ml<sup>-1</sup> MTT, and 0, 2.5, 5, 7.5, or 10 mM zanamivir was added. Cells were  
298 incubated for 2.5 hours at 37 °C, 5 % CO<sub>2</sub>. MTT-supplemented media was removed, and cells were  
299 washed twice using PBS. Formazan crystals were solubilised using isopropanol + 0.125 % (v/v) HCl,  
300 and quantified by measuring absorbance at 540 nm, reference at 630 nm using a Tecan Infinite  
301 M200 plate reader. A commercially available lactate dehydrogenase (LDH) assay, Cytotox 96  
302 (Promega) was also used to assess cell membrane permeability as a measure of viability, according  
303 to manufacturers’ instructions, with cells seeded as described for MTT assays.

## 304 **Results**

305 **SiaPG is a highly active, broad specificity sialidase, and desialylates host glycans.** The coding  
306 sequence of SiaPG without secretion signal sequence was synthesized as a codon optimised  
307 fragment and cloned into a pET21a plasmid. Expression was performed in *E. coli* BL21 (origami B),  
308 and purified via Nickel affinity chromatography to high homogeneity (supplemental figure S1). The  
309 commonly used fluorogenic 4-methylumbelliferyl-N-acetyl neuraminic acid (MUNANA) substrate was  
310 used to assess sialidase activity with liberated 4-methylumbelliferone (4-MU) measured with  
311 fluorescence change per minute used to quantify sialidase activity (Figure 1 A). We observed that  
312 SiaPG has optimal activity under acidic conditions, with highest activity observed at a pH of 5.2-5.6.  
313 However, it retained 40-50 % activity between pH 4.4 and 7.2, and ~20-30 % retained even at pH 4  
314 and 8. Whole bacterial sialidase activity of *P. gingivalis* was also assessed, finding that  $\geq$ ~70 %  
315 maximal activity was retained in the pH range 4.8-8.0, with the highest activity observed at pH 6.8,  
316 (Figure 1 B). The stronger activity of whole *P. gingivalis* sialidase in a wider pH range compared to  
317 the sialidase protein may be due to a buffering or stabilising effect of cell membranes or other  
318 components and is relevant given that subgingival GCF pH is in the neutral range.

319 We also performed kinetics experiments to enable comparison of SiaPG to other sialidases.  
320 Given the pH variations in the pathogens' ecological niche, i.e. the conditions the sialidases would  
321 encounter in the host, we evaluated sialidase activity at SiaPG-optimum (pH 5.6) as well as  
322 physiological pH (7.4) that would be present in the mouth, and in the presence and absence of  
323 additional salt (figure 2). SiaPG had the greatest catalytic efficiency ( $k_{cat}/K_M$ ) at pH 5.6 in the  
324 presence of salt ( $161.0 \mu\text{M min}^{-1}$  with 200 mM NaCl,  $124.7 \mu\text{M min}^{-1}$  without NaCl). At pH 7.4, salt had  
325 a similar impact on catalytic efficiency of SiaPG ( $49.9 \mu\text{M min}^{-1}$  with NaCl,  $36.4 \mu\text{M min}^{-1}$  without NaCl).  
326 These values are broadly in line with those previously reported for the NanH sialidase of *T. forsythia*  
327 [24], though salt had the opposite effect on NanH catalytic efficiency.

328 In addition to MUNANA, we assessed the ability of SiaPG to cleave 2-3' and 2-6' linked sialic  
329 acid, initially with the trisaccharide substrate sialyllactose (3- and 6- sialyllactose), using a TBA assay  
330 as previously described for NanH. SiaPG was capable of cleaving both linkage types (Figure 3), and  
331 although it had a much higher affinity (lower  $K_M$ ) for the 2,6 linkage than 2,3, its reaction velocity  
332 with the 2,3 version means that it has a ~50 % higher catalytic efficiencies ( $K_{cat}/K_M$ ) for the 3-  
333 sialyllactose linked sugars.

334 Desialylation of more complex and physiologically relevant glycans by SiaPG was also  
335 assessed using HPLC and mass spectrometry. SLeX is an oligosaccharide containing  $\alpha$ 2-3 linked sialic  
336 acid, and is present in numerous host niches-on the plasma membrane of various cell types and at  
337 the termini of secreted glycans. SLeX may also play a role in *P. gingivalis* pathogenesis [28]. We

338 exposed soluble SLeX to SiaPG, subjected the reaction to HPLC, and found that SLeX was efficiently  
339 desialylated by SiaPG (Figure 4A). Cleavage of  $\alpha$ 2-6 linked sialic acid by SiaPG was tested using the  
340 host-relevant FA2G2S2 (also known as A2F) glycan, a two-branched polysaccharide chain where both  
341 branches terminate with a sialic acid, which is present on a number of secreted glycoproteins  
342 including IgG. SiaPG was again capable of desialylating FA2G2S2 (Figure 4B). Notably, other peaks  
343 were observed in the chromatogram for FA2G2S2, which are likely to correspond to differently  
344 sialylated versions of the FA2G2S2 glycan, and these also appeared to be desialylated - notably the  
345 mammalian NeuGc versions. It would be interesting to test the activity of SiaPG against such NeuGc  
346 linked glycoconjugates, which the human host does not synthesize but obtains from dietary sources.

347 Finally, we wanted to test desialylation of glycans derived from a complex sialoglycoprotein  
348 by SiaPG. To this end, we chose the host glycoprotein erythropoietin (EPO) due to its possession of  
349 multiple bi-, tri- and tetra- branched glycans, the presence of  $\alpha$ 2-3 and  $\alpha$ 2-6 sialic acid linkages, and  
350 because some of its NeuAc is mono or di-O-acetylated (Neu5,9Ac, and perhaps tri-acetylated  
351 Neu5,8,9Ac). EPO was digested with SiaPG, N-glycans were procainamide labelled, and these  
352 underwent UHPLC-MS/MS (Figure 5). As expected, the UHPLC chromatogram of undigested EPO  
353 showed the presence of multiple peaks corresponding to various EPO glycans, further details and  
354 structures of these are shown in supplemental table 1. Following digestion with SiaPG, we observed  
355 a marked change in the chromatogram. The remaining peaks were investigated by MS/MS, providing  
356 evidence that SiaPG was able to cleave the sialic acid from a wide-range of glycan structures.  
357 However, this analysis also revealed the inability of SiaPG to cleave diacetylated (or triacetylated)  
358 sialic acids (Figure 5, lower 2 panels). These analyses showed that extracted ion chromatogram (EIC)  
359 corresponding to the MS2 ion for Neu5Ac trisaccharide (GlcNAc-Gal-Neu5Ac,  $m/z = \sim 657.25$ ) was not  
360 detected above background levels, while EIC corresponding to di- and tri- acetylated sialic acid  
361 trisaccharides (GlcNAc-Gal-Neu5,9Ac and GlcNAc-Gal-Neu5,8,9Ac,  $m/z = \sim 699.25$  and  $\sim 741.26$ ) were  
362 detected in high abundance (high peak intensity)- i.e. had been left uncleaved by SiaPG; a result  
363 expected given our previous studies on NanH [23].

364 **SiaPG releases Neu5Ac from mucins, an activity enhanced by the sialate-O-acetyl esterase NanS**  
365 **from *T. forsythia*.** To explore activity of SiaPG further we next tested its activity with a glycoprotein  
366 substrate relevant in the oral cavity- salivary mucin. Notably the commonly used Bovine  
367 Submaxillary mucin (BSM) used in these experiments contains many terminal sialic acids that have  
368 the second O-acetyl group, i.e. contain Neu5,9Ac [29]. Our previous data on NanH [23] and SiaPG  
369 (this study) indicate terminal Neu5,9Ac is resistant to cleavage by periodontal sialidases. To counter  
370 this, some bacteria express sialate-O-acetyl esterases, such as NanS from *T. forsythia*, which remove

371 the second acetylation (forming Neu5Ac), and rendering the sialic acid susceptible to sialidase  
372 cleavage. Indeed, we previously demonstrated that *T. forsythia* NanS enhances NanH sialidase  
373 activity on Neu5,9Ac terminal sugars and may act to aid sialidases from other species in harvesting  
374 sialic acid [23]. To test the hypothesis that *T. forsythia* may act to enhance SiaPG activity we  
375 performed sialic acid release assays on BSM. The data showed that NanS enhanced sialic acid release  
376 by SiaPG from BSM by ~2.5 -fold (from 302 to 746 pmol/min) (Figure. 7).

377 **Zanamivir more efficiently inhibits sialidase activity of SiaPG and whole *P. gingivalis* than sialidase**  
378 **activity of *T. forsythia* NanH and whole *T. forsythia*.** As outlined, one aim of this study was to assess  
379 the ability of a safe and FDA-approved drug in its ability to potentially reduce virulence of the  
380 keystone periodontal pathogen, *P. gingivalis*. Therefore we assessed the impact of zanamivir on the  
381 activity of whole *P. gingivalis* and another periodontal pathogen, *T. forsythia*, as well as their purified  
382 sialidases using the MUNANA assay as described above. Both pathogens and purified sialidases  
383 displayed decreased sialidase activity as zanamivir concentration was increased (Figure 6 A). The  
384 decrease in activity was far more drastic for *P. gingivalis*, with a decrease in activity of ~70 % in the  
385 presence of 10 mM zanamivir, compared to *T. forsythia* which only showed a decrease of ~25 %  
386 (Figure 6 B). This apparent difference in efficacy for the two sialidases was confirmed by establishing  
387 the IC50 of zanamivir for purified SiaPG and NanH (Figure 6 B), where zanamivir displayed a greater  
388 inhibitory effect on SiaPG (369  $\mu$ M) than NanH (6130  $\mu$ M). These data were further enhanced when  
389 we observed that zanamivir also inhibited sialidase activity in the context of removal of sialic acid  
390 from mucin (Figure 7). There was no effect on NanS sialate-*O*-acetyltransferase activity alone (data not  
391 shown).

392 ***P. gingivalis* biofilms on host sialoglycans are sialidase-dependent and disrupted by zanamivir.** *P.*  
393 *gingivalis* was cultured in microtitre plates, where well surfaces were coated with mucin (BSM),  
394 saliva (pooled human saliva), or serum (FCS) in the presence or absence of 10 mM zanamivir. Total  
395 growth (Figure 8 A) of *P. gingivalis* in the mucin-coated condition was significantly reduced in the  
396 presence of zanamivir, from OD600 0.21 to 0.11 ( $p < 0.001$ ) i.e. zanamivir reduced total growth of *P.*  
397 *gingivalis* in mucin-coated conditions by approximately half. In the presence of the other  
398 glycoprotein-coated conditions (saliva and serum) there was a trend towards small reductions in  
399 total growth in the presence of zanamivir but these did not reach statistical significance. Biofilm  
400 formation (normalised to total growth-optical density) of *P. gingivalis* (Figure 8 B) was also reduced  
401 when grown on mucin coated surfaces (30-40 % reduction,  $p < 0.01$ ), indicating that biofilm  
402 formation on these surfaces was inhibited by zanamivir. Notably we also saw a consistent small

403 reduction on serum, but total growth (OD600) standardised to biofilm formation (bacteria ml<sup>-1</sup>) of  
404 cultures grown on human saliva-coated surfaces was too variable to make conclusions.

405 In support of our evidence that sialidase is important when *P. gingivalis* grows on mucin coated  
406 surfaces (as would often be the case *in vivo*), we also tested the effect of sialidase activity in this  
407 regard in a related *P. gingivalis* strain – 381 (Pg381). For this purpose, a *siaPG* deletion mutant of *P.*  
408 *gingivalis* 381 and its complemented strain were constructed (Pg381Δ*siaPG* and Δ*siaPG*<sup>+</sup>).  
409 Pg381Δ*siaPG* showed no sialidase activity as judged from lack of fluorescence on incubation with  
410 MUNANA, while the sialidase activity was restored in the complemented strain Δ*siaPG*<sup>+</sup> (supplemental  
411 figure S2). In biofilm assays, we observed a 2-fold reduction in biofilm growth in Pg381Δ*siaPG*  
412 (relative to the WT) on mucin coated surfaces, with this phenotype complemented by provision of  
413 the *SiaPG* gene in the mutant (Δ*siaPG*<sup>+</sup>, figure. 9). These data expand our view of the role of sialidase  
414 to a range of *P. gingivalis* strains and suggest it may be true across this species.

415 **SiaPG releases 3- and 6- linked sialic acid from oral epithelial cells and is inhibited by zanamivir.**

416 Studies of mutant strains and purified enzymes have shown that the well-studied *T. forsythia* NanH  
417 can desialate oral epithelial cells [22, 24], while *SiaPG* mutant strains have been used to highlight *P.*  
418 *gingivalis* sialidase-mediated release of sialic acid from erythrocytes [18]. In order to test the effect  
419 of *SiaPG* on physiologically relevant oral epithelial cells, we stained the OSCC line H357 with the  
420 lectins SNA and MAA enabling fluorescent imaging of cell surface α2-3 and α2-6- linked sialic acid.  
421 Exposure of epithelial cells to *SiaPG* (and *T. forsythia* NanH) was successful in desialylating cell  
422 surfaces (this had been shown previously for NanH [22]), while 10 mM zanamivir inhibited  
423 desialylation in the case of *SiaPG*, but not NanH (figure 10, supplemental figure S3).

424 **Zanamivir inhibits periodontal pathogen-host cell association during monospecies infection.** One  
425 established aspect of *P. gingivalis* virulence is its ability to invade and reside within oral epithelial  
426 cells. To this end we performed antibiotic protection assays to establish whether zanamivir had any  
427 potential effect on host cell interaction and invasion. However, the effects of zanamivir on bacterial  
428 and human cell viability had to be established. To this end, oral epithelial cells were subjected to 10  
429 mM zanamivir under antibiotic protection assay conditions, illustrating no effect of zanamivir on  
430 either membrane integrity (assayed by LDH) or cellular activity/ viability (via MTT assay)  
431 (supplemental figure S4). Similarly, we incubated *P. gingivalis*, *T. forsythia* and *F. nucleatum* with  
432 zanamivir under antibiotic protection assay conditions (2.5 hours in tissue culture medium), before  
433 obtaining cfu counts, and revealed no detrimental effect of zanamivir on viability of any of these  
434 species (supplemental figure S5).

435 Next we performed antibiotic protection assays on two oral epithelial cell lines, namely the OSCC cell  
436 line H357- a frequently used model for oral epithelium-bacteria interactions in our laboratory [30,  
437 31] and normal immortalised oral epithelial cell line OKF6 [32, 33]. In addition to *P. gingivalis* we  
438 also tested the effect of zanamivir on two other key periodontal pathogens- namely *T. forsythia* and  
439 *F. nucleatum* subsp. *nucleatum*. For all three pathogens, in both cell lines, zanamivir significantly  
440 reduced one or more aspects of host-bacteria association in both cell lines (figure 11). For *T.*  
441 *forseythia*, attachment, invasion, and total association (the sum of attached and invaded bacteria)  
442 were all significantly reduced in both cell lines; from 3.2 to 1.0 %, 2.5 to 0.3 %, and 5.8 to 1.4 % in  
443 OKF6 cells, and 4.6 to 1.2 %, 3.4 to 1.6 %, and 8.0 to 2.8 % in H357 cells (figure 11 A). For *P.*  
444 *gingivalis*, attachment, invasion, and total association were significantly reduced in OKF6 cells; from  
445 0.9 to 0.1 %, 0.7 to 0.1 %, and 1.7 to 0.2 %, however in the H357 cell line, only invasion was  
446 significantly reduced, from 4.5 to 1.8 % (figure 11 B). Finally, for *F. nucleatum*, invasion and total  
447 association were significantly reduced in OKF6 cells; from 4.6 % to 1.3 %, and 5.6 to 2.6 %. For H357  
448 cells attachment and total association were significantly reduced 21.8 % to 7.2 %, and 36.6 % to 18.2  
449 % (figure 11 C).

450 To support the notion that sialidase activity is important for bacteria-host cell association, rather  
451 than disruption of other processes by the presence of zanamivir, the human gingival cell line OBA-9  
452 was exposed to *P. gingivalis* 381 (Pg381) and a *siaPG* deficient mutant (Pg381 $\Delta$ *siaPG*). Exposure to  
453 the latter strain was performed without or with exogenous SiaPG . Pg381 $\Delta$ *siaPG* displayed  
454 significantly decreased association with host cells relative to the parent Pg381, which was restored  
455 by the presence of exogenous SiaPG in a concentration dependent manner (supplemental figure S6):  
456 While 100  $\mu$ g ml<sup>-1</sup> exogenous recombinant SiaPG resulted in partial restoration of host-bacteria  
457 association of Pg381 $\Delta$ *siaPG* (WT; 0.50 %, Pg381 $\Delta$ *siaPG* ; 0.15 %, Pg381 $\Delta$ *siaPG*+100  $\mu$ g SiaPG ; 0.26),  
458 200  $\mu$ g/ml SiaPG resulted in complete restoration of host-bacterial association Pg381 (0.58 %).

459 **Zanamivir inhibits attachment and invasion of oral epithelial cells during infection with multiple**  
460 **periodontal pathogens.** To at least partially mimic the *in vivo* situation, where none of these species  
461 exist in isolation, we performed antibiotic protection assays where multiple periodontal pathogens  
462 were used to infect cells. This is particularly relevant during host cell association, since periodontal  
463 pathogens have been shown to act in synergy during attachment and invasion [34–36]. MOI was  
464 maintained at 1:100 host cells: bacteria, so for infections using two species, the ratio was 1:50:50  
465 (host cells: species 1: species 2), and for infections with all three species, the ratio was 1:33:33:33  
466 (host cells: species 1: species 2: species 3). *T. forsythia*, *P. gingivalis*, and *F. nucleatum* were used in a  
467 variety of combinations to infect epithelial cells. In addition to quantifying the numbers of all

468 bacteria-not distinguishing between species during an assay-the levels of each individual species in a  
469 given assay could be enumerated by colony counting on agar plates, since the colony morphologies  
470 of *T. forsythia*, *F. nucleatum*, and *P. gingivalis* are distinct from each other (supplemental figure S7).  
471 All possible combinations were tested in this way. For ease of discussion, only the total number of  
472 bacteria in each combination are described here, with complete results for each individual species  
473 provided in supplemental figures S8-S11. For *T. forsythia* and *F. nucleatum* co-infection, zanamivir  
474 significantly reduced both invasion and total association of bacteria with host cells, from 7.4 to 1.8  
475 %, and 19.6 to 7.6 % ( $p < 0.01$  and  $p < 0.05$ ), respectively (Figure 12 A). For *T. forsythia* and *P. gingivalis*  
476 co-infection, the variation between experiments meant that none of the reductions were statistically  
477 significant (where  $p < 0.05$ , Figure 12 B), i.e. attachment was reduced from 12.1 to 0.8 % ( $p = 0.076$ ),  
478 invasion from 2.8 to 1.4 % ( $p = 0.25$ ), and total association from 14.4 to 2.5 % ( $p = 0.062$ ). For *F.*  
479 *nucleatum* and *P. gingivalis*, zanamivir significantly reduced attachment, invasion, and total  
480 association of bacteria with host cells, from 1.9 to 0.8 % ( $p < 0.05$ ), 4.0 to 1.56 % ( $p < 0.05$ ), and 5.9  
481 to 2.4 % ( $p < 0.01$ ), respectively (figure 12 C). Finally, all three species (i.e. *T. forsythia*, *F. nucleatum*  
482 and *P. gingivalis*) were infected into the cells as a three-species community. Here, strikingly,  
483 zanamivir significantly reduced attachment, invasion, and total association of bacteria with host  
484 cells, from 17.7 to 7.7 % ( $p = < 0.001$ ), 9.6 to 7.15 % ( $p = < 0.05$ ), and 26.14 to 14.6 % ( $p = < 0.001$ ),  
485 respectively (figure 12 D); indicating this approach might have impact on cellular interaction *in vivo*.

## 486 Discussion

487 In this study we characterised the activity of the sialidase (SiaPG) from *P. gingivalis* on a number of  
488 glycan and proteinaceous substrates, including relevant host sialoglycans SleX, FA2G2S2 and EPO,  
489 and establishing activity across a range of pH values. During these studies, it became apparent that  
490 SiaPG could cleave both  $\alpha 2$ -3 and  $\alpha 2$ -6 linked Neu5Ac, but not diacetylated Neu5,9Ac. These data  
491 also agreed with low sialic acid release from the heavily diacetylated BSM protein, and this activity  
492 being enhanced by coincubation with an enzyme capable of removing O-acetyl groups on sialic acid  
493 residues - namely the NanS sialate-O-acetyl esterase from the fellow oral bacterium *T. forsythia* [23].  
494 We hypothesise that *in vivo* NanS enhances the ability of *P. gingivalis* to cleave sialic acid from  
495 glycoproteins - although given the fact that *P. gingivalis* does not produce its own esterase or utilise  
496 sialic acid for nutrition we can only postulate that somehow removal of sialic acid opens up sites for  
497 adhesion to oral surfaces, or might modulate immune responses mediated by Siglecs (sialic acid-  
498 binding immunoglobulin-like lectins) or allow *P. gingivalis* to access underlying sugars or the protein  
499 component of the glycoproteins themselves, and may explain synergies between these organisms  
500 observed by others [37–39].

501 We tested the ability of zanamivir to inhibit SiaPG and the previously characterised NanH sialidase  
502 from another red complex pathogen, *T. forsythia*. While the inhibition (IC50) of SiaPG activity on  
503 MUNANA was determined to be within the micromolar range (~350  $\mu$ M), this was not the case for *T.*  
504 *for sythia*, which required >6 mM zanamivir to reduce its activity by half. A similar trend was also  
505 seen for whole bacteria. The relatively low efficacy of zanamivir for some bacterial sialidases is  
506 observed in other studies where sialidases from the pathogens *S. pneumoniae* and *Gardnerella*  
507 *vaginalis* are apparently only inhibited to limited extents [40, 41]. Nevertheless, here we showed  
508 that *P. gingivalis* sialidase was effectively inhibited by zanamivir. At present we have no mechanistic  
509 explanation for the variation between the two sialidases, but postulate it may result from structural  
510 differences, despite both possessing typical catalytic GH33 domains with predicted 6-blade propeller  
511 structures the sialidases only share 23 % amino acid sequence identity.

512 Given this, and the ability of SiaPG to cleave sialic acid from complex glycans (FA2G2S2, EPO), we  
513 assessed the ability of SiaPG to remove sialoglycans from oral epithelial cells, illustrating removal in  
514 both cases and highlighting the broad glycan specificity of this enzyme and the ability of zanamivir to  
515 affect this process. As shown previously, NanH was also capable of desialylating oral epithelial cells  
516 [22].

517 Considering the ability of zanamivir to inhibit *P. gingivalis* sialidase activity, *in vitro* virulence models  
518 were carried out. It has been shown previously that NanH is key during biofilm formation in *T.*  
519 *for sythia*, and that sialidase inhibitors are also detrimental to *T. forsythia* biofilms [42]. We observed  
520 that sialidase inhibitors decreased *P. gingivalis* biofilm formation on host glycoprotein sources,  
521 significantly on saliva and mucin. In addition, biofilm formation of sialidase deficient *P. gingivalis* on  
522 mucin was reduced compared to its parent, and restored upon complementation. Biofilms of  
523 sialidase deficient *P. gingivalis* are also reduced on plastic surfaces [17]. There are various  
524 mechanisms by which sialidase activity may contribute to *P. gingivalis* biofilm formation. Possibilities  
525 include decreased proteolysis and subsequent nutrient deficiency or an inability to attach to cleaved  
526 proteins, since sialylation may protect against proteolytic activity [43]. Interference with the *P.*  
527 *gingivalis* capsule is also possible, sialidase expression appears to be important for *P. gingivalis*  
528 capsular synthesis, mutants deficient in SiaPG show reduced capsule formation [17, 18], and yet loss  
529 of the capsule has been shown to enhance biofilm formation [44], thus, we might expect zanamivir  
530 (or sialidase knockout) to enhance biofilm formation, but here we observed the opposite, possibly  
531 because non-capsulated (fimbriated) strains were tested. In any case, we cannot rule out the  
532 possibility that sialidase inhibition may interfere with capsular structure or interactions in the case of  
533 *P. gingivalis* strains which are encapsulated. Finally, maturation and processing of gingipains-

534 proteases central to *P. gingivalis* virulence and asacharolytic nutrition-is also altered in sialidase  
535 deficient mutants [18]. Zanamivir may impact biofilm formation through any, or all, of these  
536 mechanisms. It would be particularly interesting to assess the impact of zanamivir on mixed-species  
537 biofilms, and in addition to direct impacts on sialic acid-mediated interactions and any indirect  
538 effects that may result from sialidase inhibition. For example, it has been previously shown that  
539 lysine gingipains (Kgp) of *P. gingivalis* mediate *T. forsythia* levels in mixed species biofilms [45], and .  
540 given that sialylation may influence protease access to protein backbones, inhibition of *P. gingivalis*  
541 sialidase may also impact the activity of Kgp, subsequently reproducing the detrimental effect of Kgp  
542 deficiency on *T. forsythia* abundance. Similarly, it has been noted that *T. forsythia* surface S-layer  
543 glycans play a potential role in localisation with *P. gingivalis* within polymicrobial biofilms [46].  
544 These glycans contain terminal nonulosonic analogues of sialic acid (pseudaminic and legianaminic  
545 acids) and it is possible that Zanamivir may influence these interactions as a glycan mimic.

546 Given that periodontal pathogen sialidases have been shown to be important during host cell  
547 association [17, 18, 22, 42] and zanamivir inhibited host cell surface desialylation by SiaPG, but not *T.*  
548 *for sythia* NanH, it might be expected that zanamivir would decrease attachment and invasion of  
549 host cells by *P. gingivalis* but not *T. for sythia*. Surprisingly, host cell association was greatly inhibited  
550 in the case of both organisms, and in the sialidase negative *F. nucleatum* [13]. Of note here is that  
551 while our data re-emphasize the role of sialidase in the equivalent *P. gingivalis* capsulated W83  
552 strain [18], indicating that this phenotype is widespread in *P. gingivalis*, it would be of interest to  
553 establish whether zanamavir has the same effect on capsulated strains. It is also possible that other  
554 periodontal pathogen virulence factors are inhibited by zanamivir. For example, the adhesin FadA is  
555 highly conserved among oral fusobacteria, and considered important for association with oral  
556 epithelial cells [47] and has been shown to bind cell surface E-selectin, whose native ligand is a  
557 sialoglycan (sialyl lewis A/X), so perhaps a sialic acid analogue might interfere with FadA-host cell  
558 surface interactions.

559 Although the monospecies antibiotic protection assays hinted at the usefulness of zanamivir as an  
560 anti-virulence therapeutic, periodontitis is mediated by a dysbiotic polymicrobial community.  
561 Therefore, we performed mixed species antibiotic protection assays with combinations of all three  
562 of the periodontal pathogens from the monospecies antibiotic protection assays. Importantly,  
563 zanamivir influenced invasion in the triple-species infection model with *F. nucleatum*, *P. gingivalis*,  
564 and *T. for sythia*. Despite evidence of synergy in invasive capability reported in the literature [34, 36,  
565 48] we were surprised zanamivir effected all species in these assays, given that *F. nucleatum* has no  
566 sialidase and *T. for sythia* sialidase is only weakly inhibited by zanamivir. One explanation might be

567 that only a modest reduction in sialidase activity can reduce invasion for *T. forsythia*. However,  
568 zanamivir acts on host sialidases, in particular Neu1 and Neu3, which contribute to the immune  
569 response to bacteria via TLRs, where host sialidases are mobilised to the plasma membrane where  
570 they activate TLRs 2-, 3- and 4- [49-51], and zanamivir (and other sialidase inhibitors) has been  
571 shown to inhibit TLR activation by LPS [52]. Inhibition of host cell sialidases by zanamivir may  
572 therefore affect the cell surface charge and glycosylation state of receptors involved in bacterial  
573 adhesion and invasion. Indeed our data may suggest that there are host and bacterial sialidase  
574 dependent events that not only warrant further study but make a strong case for the potential of  
575 these inhibitors to affect periodontal disease pathogenesis, since they may have dual action on host  
576 and bacterial processes.

## 577 **Conclusion**

578 In summary, we further characterised the sialidase of *P. gingivalis*, and provided evidence  
579 advocating for the development of sialidase inhibitors as therapeutics for periodontitis-and other  
580 diseases-where bacterial sialidases play key roles in virulence. Zanamivir was capable of inhibiting  
581 sialidase activity and virulence mechanisms of *P. gingivalis*, most prominently host cell association.  
582 However, our study raises several questions and directions for further work, most notably that host  
583 as well as bacterial sialidase may influence interactions more than currently understood. Ultimately,  
584 sialidase inhibition represents a potential novel therapy for periodontal and other diseases, and  
585 merits further investigation. Finally, zanamivir is a safe and efficacious drug for treatment of  
586 influenza, but clearly only inhibits bacterial sialidases relatively weakly ( $\mu\text{M}$  – $\text{mM}$  range). However,  
587 its effectiveness in this study suggests that the development of more potent and selective inhibitors  
588 of bacterial sialidase should be a focus in upcoming years as they may hold potential as a safe and  
589 efficacious treatment in periodontal and other diseases.

## 590 **Author statements**

591 **Funding:** AF and MS were funded by a BBSRC iCASE studentships (BB/K501098/1, BB/M01570X/1),  
592 while CP was funded by a grant from the Dunhill Medical Trust to GS (DMT-R185/0211). We  
593 acknowledge the funding form NIH grant DE14749 to AS and William M. Feagans Endowed Chair  
594 Research Fund, University at Buffalo School of Dental Medicine to KH.

595 **Conflict of Interest:** We declare no conflicts of interest, besides the provision of zanamivir by  
596 GlaxoSmithKline (GSK), Stevenage, UK, and AF was sponsored by a BBSRC iCASE studentship  
597 (BB/K501098/1) in partnership with GSK.

598 **Author contributions:** AF, GS, JP and DB devised the concept of the work. AF, MS, PU, DS, KH and CP  
599 performed aspects of lab analysis. AF, GS and AS drafted and wrote the manuscript. All authors  
600 contributed to editing of the paper.

## 601 **Bibliography**

- 602 1. **Hajishengallis G, Darveau RP, Curtis MA.** The keystone-pathogen hypothesis. *Nat Rev*  
603 *Microbiol* 2012;10:717–725.
- 604 2. **Meuric V, Le Gall-David S, Boyer E, Acuña-Amador L, Martin B, et al.** Signature of microbial  
605 dysbiosis in periodontitis. *Appl Environ Microbiol* 2017;83:1–13.
- 606 3. **Socransky SS, Haffajee a D, Cugini M a, Smith C, Kent RL.** Microbial complexes in subgingival  
607 plaque. *J Clin Periodontol* 1998;25:134–44.
- 608 4. **Ximénez-Fyvie L a, Haffajee a D, Socransky SS.** Comparison of the microbiota of supra- and  
609 subgingival plaque in health and periodontitis. *J Clin Periodontol* 1999;27:648–57.
- 610 5. **Muniz FWMG, De Oliveira CC, De Sousa Carvalho R, Moreira MMSM, De Moraes MEA, et al.**  
611 Azithromycin: A new concept in adjuvant treatment of periodontitis. *Eur J Pharmacol*  
612 2013;705:135–139.
- 613 6. **Colombo AP, Boches SK, Cotton SL, Goodson JM, Kent R, et al.** Comparisons of subgingival  
614 microbial profiles of refractory periodontitis, severe periodontitis, and periodontal health  
615 using the human oral microbe identification microarray. *J Periodontol* 2009;80:1132–1421.
- 616 7. **Lohr G, Beikler T, Hensel A.** Inhibition of in vitro adhesion and virulence of *Porphyromonas*  
617 *gingivalis* by aqueous extract and polysaccharides from *Rhododendron ferrugineum* L. A new  
618 way for prophylaxis of periodontitis? *Fitoterapia* 2015;107:105–113.
- 619 8. **Kariu T, Nakao R, Ikeda T, Nakashima K, Potempa J, et al.** Inhibition of gingipains and  
620 *Porphyromonas gingivalis* growth and biofilm formation by prenyl flavonoids. *J Periodontal*  
621 *Res* 2016;52:89–96.
- 622 9. **Huq NL, Seers CA, Toh ECY, Dashper SG, Slakeski N, et al.** Propeptide-Mediated Inhibition of  
623 Cognate Gingipain Proteinases. *PLoS One* 2013;8:e65447–e65447.
- 624 10. **Dominy SS, Lynch C, Ermini F, Benedyk M, Marczyk A, et al.** *Porphyromonas gingivalis* in  
625 Alzheimer’s disease brains: Evidence for disease causation and treatment with small-  
626 molecule inhibitors. *Sci Adv* 2019;5:eaau3333.

- 627 11. **Parker D, Soong G, Planet P, Brower J, Ratner AJ, et al.** The NanA neuraminidase of  
628 Streptococcus pneumoniae is involved in biofilm formation. *Infect Immun* 2009;77:3722–  
629 3730.
- 630 12. **Galen JE, Ketley JM, Fasano A, Richardson SH, Wasserman SS, et al.** Role of Vibrio cholerae  
631 Neuraminidase in the Function of Cholera Toxin. *Infect Immun* 1992;60:406–415.
- 632 13. **Stafford G, Roy S, Honma K, Sharma A.** Sialic acid, periodontal pathogens and Tannerella  
633 forsythia: Stick around and enjoy the feast! *Mol Oral Microbiol* 2012;27:11–22.
- 634 14. **Palmer RJ.** Composition and development of oral bacterial communities. *Periodontol 2000*  
635 2014;64:20–39.
- 636 15. **Frey AM, Ansbro K, Kamble NS, Pham TK, Stafford GP.** Characterisation and pure culture of  
637 putative health-associated oral bacterium BU063 ( Tannerella sp . HOT-286 ) reveals presence  
638 of a potentially novel glycosylated S-layer. *FEMS Letters* 2018;365:1–8.
- 639 16. **Roy S, Honma K, Douglas I, Sharma A, Stafford GP, et al.** Role of sialidase in glycoprotein  
640 utilisation by Tannerella forsythia. *Microbiology* 2011;157:3195–3202.
- 641 17. **Li C, Kurniyati, Hu B, Bian J, Sun J, et al.** Abrogation of neuraminidase reduces biofilm  
642 formation, capsule biosynthesis, and virulence of Porphyromonas gingivalis. *Infect Immun*  
643 2012;80:3–13.
- 644 18. **Aruni W, Vanterpool E, Osbourne D, Roy F, Muthiah A, et al.** Sialidase and  
645 sialoglycoproteases can modulate virulence in Porphyromonas gingivalis. *Infect Immun*  
646 2011;79:2779–2791.
- 647 19. **Kurniyati K, Zhang W, Zhang K, Li C.** A surface-exposed neuraminidase affects complement  
648 resistance and virulence of the oral spirochaete Treponema denticola. *Mol Microbiol*  
649 2013;89:842–856.
- 650 20. **Duran-Pinedo AE, Chen T, Teles R, Starr JR, Wang X, et al.** Community-wide transcriptome of  
651 the oral microbiome in subjects with and without periodontitis. *ISME J* 2014;8:1659–72.
- 652 21. **Gul SS, Griffiths GS, Stafford GP, Al-Zubidi MI, Rawlinson A, et al.** Investigation of a Novel  
653 Predictive Biomarker Profile for the Outcome of Periodontal Treatment. *J Periodontol*. Epub  
654 ahead of print 2017. DOI: 10.1902/jop.2017.170187.
- 655 22. **Honma K, Mishima E, Sharma A.** Role of tannerella forsythia NanH sialidase in epithelial cell

- 656 attachment. *Infect Immun* 2011;79:393–401.
- 657 23. **Phansopa C, Kozak RP, Liew LP, Frey AM, Farmilo T, et al.** Characterization of a sialate-O-  
658 acetylesterase (NanS) from the oral pathogen *Tannerella forsythia* that enhances sialic acid  
659 release by NanH, its cognate sialidase. *Biochem J* 2015;472:157–167.
- 660 24. **Frey AM, Satur MJ, Phansopa C, Parker JL, Bradshaw D, et al.** Evidence for a novel  
661 Carbohydrate Binding Module (CBM) of *Tannerella forsythia* NanH sialidase, key to  
662 interactions at the host-pathogen interface. *Biochem J* 2018;20170592:BCJ20170592.
- 663 25. **Honma K, Mishima E, Inagaki S, Sharma A.** The OxyR homologue in *Tannerella forsythia*  
664 regulates expression of oxidative stress responses and biofilm formation. *Microbiology*  
665 2009;155:1912–1922.
- 666 26. **Royle L, Mattu TS, Hart E, Langridge JI, Merry AH, et al.** An analytical and structural database  
667 provides a strategy for sequencing O-glycans from microgram quantities of glycoproteins.  
668 *Anal Biochem* 2002;304:70–90.
- 669 27. **Schindelin J, Arganda-Carreras I, Frise E, Kaynig V, Longair M, et al.** Fiji: An open-source  
670 platform for biological-image analysis. *Nat Methods* 2012;9:676–682.
- 671 28. **Komatsu T, Nagano K, Sugiura S, Hagiwara M, Tanigawa N, et al.** E-selectin mediates  
672 *Porphyromonas gingivalis* adherence to human endothelial cells. *Infect Immun*  
673 2012;80:2570–2576.
- 674 29. **Varki A, Diaz S.** A Neuraminidase from *Streptococcus sanguis* That Can Release O-acetylated  
675 Sialic Acids. *J Biol Chem* 1983;258:12465–12471.
- 676 30. **Suwannakul S, Stafford GP, Whawell SA, Douglas CWI.** Identification of bistable populations  
677 of *Porphyromonas gingivalis* that differ in epithelial cell invasion. *Microbiology*  
678 2010;156:3052–3064.
- 679 31. **Al-Taweel FB, Ian Douglas CW, Whawell SA.** The periodontal pathogen *Porphyromonas*  
680 *gingivalis* preferentially interacts with oral epithelial cells in S phase of the cell cycle. *Infect*  
681 *Immun* 2016;84:1966–1974.
- 682 32. **Dickson MA, Hahn WC, Ino Y, Ronfard V, Wu JY, et al.** Human keratinocytes that express  
683 hTERT and also bypass a p16(INK4a)-enforced mechanism that limits life span become  
684 immortal yet retain normal growth and differentiation characteristics. *Mol Cell Biol*  
685 2000;20:1436–47.

- 686 33. **Naylor KL, Widziolek M, Hunt S, Conolly M, Hicks M, et al.** Role of OmpA2 surface regions of  
687 Porphyromonas gingivalis in host – pathogen interactions with oral epithelial cells. *Microbiol*  
688 *Open* 2017;1–11.
- 689 34. **Saito A, Kokubu E, Inagaki S, Imamura K, Kita D, et al.** Porphyromonas gingivalis entry into  
690 gingival epithelial cells modulated by Fusobacterium nucleatum is dependent on lipid rafts.  
691 *Microb Pathog* 2012;53:234–242.
- 692 35. **Inagaki S, Onishi S, Kuramitsu HK, Sharma A.** Porphyromonas gingivalis vesicles enhance  
693 attachment, and the leucine-rich repeat BspA protein is required for invasion of epithelial  
694 cells by ‘Tannerella forsythia’. *Infect Immun* 2006;74:5023–5028.
- 695 36. **Kirschbaum M, Schultze-Mosgau S, Pfister W, Eick S.** Mixture of periodontopathogenic  
696 bacteria influences interaction with KB cells. *Anaerobe* 2010;16:461–468.
- 697 37. **Sharma A, Inagaki S, Sigurdson W, Kuramitsu HK.** Synergy between Tannerella forsythia and  
698 Fusobacterium nucleatum in biofilm formation. *Oral Microbiol Immunol* 2005;20:39–42.
- 699 38. **Settem RP, El-Hassan AT, Honma K, Stafford GP, Sharma A.** Fusobacterium nucleatum and  
700 tannerella forsythia induce synergistic alveolar bone loss in a mouse periodontitis model.  
701 *Infect Immun* 2012;80:2436–2443.
- 702 39. **Tan KH, Seers CA, Dashper SG, Mitchell HL, Pyke JS, et al.** Porphyromonas gingivalis and  
703 Treponema denticola Exhibit Metabolic Symbioses. *PLoS Pathog*;10. Epub ahead of print  
704 2014. DOI: 10.1371/journal.ppat.1003955.
- 705 40. **Govinden G, Naylor JLPKL, Anumba AMFDOC, Stafford GP.** Inhibition of sialidase activity and  
706 cellular invasion by the bacterial vaginosis pathogen Gardnerella vaginalis. *Arch Microbiol*  
707 2018;200:1129–1133.
- 708 41. **Walther E, Richter M, Xu Z, Kramer C, von Grafenstein S, et al.** Antipneumococcal activity of  
709 neuraminidase inhibiting artocarpin. *Int J Med Microbiol* 2015;305:289–297.
- 710 42. **Roy S, Honma K, Ian Douglas CW, Sharma A, Stafford GP.** Role of sialidase in glycoprotein  
711 utilization by Tannerella forsythia. *Microbiology* 2011;157:3195–3202.
- 712 43. **Lewis WG, Robinson LS, Perry J, Bick JL, Peipert JF, et al.** Hydrolysis of Secreted  
713 Sialoglycoprotein Immunoglobulin A (IgA) in ex Vivo and Biochemical Models of Bacterial. *J*  
714 *Biol Chem* 2012;287:2079–2089.

- 715 44. **Davey ME, Duncan MJ.** Enhanced Biofilm Formation and Loss of Capsule Synthesis : Deletion  
716 of a Putative Glycosyltransferase in *Porphyromonas gingivalis*. *J Bacteriol* 2006;188:5510–  
717 5523.
- 718 45. **Bao K, Belibasakis G, Thurnheer T, Aduse-Opoku J, Curtis M et al.** Role of *Porphyromonas*  
719 *gingivalis* gingipains in multi-species biofilm formation. *BMC Microbiol* 2014;14:1-8.
- 720 46. **Bloch S, Thurnheer T, Murakami Y, Belibasakis G, Schäffer C, et al.** Behavior of two  
721 *Tannerella forsythia* strains and their cell surface mutants in multispecies oral biofilms. *Mol*  
722 *Oral Microbiol* 2017;32:5:404-418.
- 723 47. **Han YW, Ikegami A, Rajanna C, Kawsar HI, Zhou Y, et al.** Identification and Characterization  
724 of a Novel Adhesin Unique to Oral Fusobacteria. *J Bacteriol* 2005;187:5330–5340.
- 725 48. **Saito A, Inagaki S, Ishihara K.** Differential ability of periodontopathic bacteria to modulate  
726 invasion of human gingival epithelial cells by *Porphyromonas gingivalis*. *Microb Pathog*  
727 2009;47:329–333.
- 728 49. **Stamatos NM, Carubelli I, van de Vlekkert D, Bonten EJ, Papini N, et al.** LPS-induced  
729 cytokine production in human dendritic cells is regulated by sialidase activity. *J Leukoc Biol*  
730 2010;88:1227–1239.
- 731 50. **Hata K, Koseki K, Yamaguchi K, Moriya S, Suzuki Y, et al.** Limited inhibitory effects of  
732 oseltamivir and zanamivir on human sialidases. *Antimicrob Agents Chemother* 2008;52:3484–  
733 3491.
- 734 51. **Amith SR, Jayanth P, Franchuk S, Finlay T, Seyrantepe V, et al.** Neu1 desialylation of sialyl  $\alpha$ -  
735 2,3-linked  $\beta$ -galactosyl residues of TOLL-like receptor 4 is essential for receptor activation and  
736 cellular signaling. *Cell Signal* 2010;22:314–324.
- 737 52. **Amith SR, Jayanth P, Franchuk S, Siddiqui S, Seyrantepe V, et al.** Dependence of pathogen  
738 molecule-induced Toll-like receptor activation and cell function on Neu1 sialidase. *Glycoconj J*  
739 2009;26:1197–1212.

740

741

742

743

744

745 Figure legends:

746

747 **Figure 1. pH optima of *P. gingivalis* whole cell sialidase activity and purified recombinant SiaPG.**

748 MUNANA was incubated with SiaPG for 1 minute or *P. gingivalis* (ATCC 33277) for 1 hour, in a variety  
749 of buffers with variable pH. Reactions were halted and the pH equalised by addition of an excess of  
750 sodium carbonate-bicarbonate buffer, pH 10.5. Sialidase activity catalysed the production of 4-MU  
751 from MU-NANA, which was quantified by measuring fluorescence of the reactions at excitation and  
752 emission wavelengths of 350 and 450 nm. A) SiaPG (B) *P. gingivalis*. Data shown represent the  
753 mean of one experiment where each condition was repeated three times. Error bars = S.E.M.

754 **Figure 2. Reaction kinetics of MUNANA and SiaPG under different conditions.** Variable

755 concentrations of MUNANA were exposed to SiaPG, under different pH and salinity conditions.  
756 Reactions were quenched by addition of pH 10.5 buffer at 1, 2, and 3 min, and the rate of 4-MU  
757 release determined by application of a 4-MU standard curve. A) Michaelis–Menten plot, rate of 4-  
758 MU release ( $V_0$ ,  $\mu\text{mol MU released min}^{-1} \text{mg}^{-1} \text{SiaPG}$ ), plotted against [MUNANA] ( $\mu\text{M}$ ) using Prism 7  
759 (GraphPad). Error bars = SD (B) Table summarising Michaelis-Menten reaction kinetics and catalytic  
760 efficiency of SiaPG and MU-NANA, the table includes the  $k_{cat}$  (4-MU release  $\text{min}^{-1}$ ), and  $k_{cat}/K_M$  ( $\mu\text{M}$   
761  $\text{min}^{-1}$ ). Data shown represent the mean ( $\pm$  S.D.) of one experiment, where each condition was  
762 repeated three times per experiment.

763 **Figure 3. Reaction kinetics of 3- or 6- sialyllactose and SiaPG under different conditions.** Variable

764 concentrations of sialyllactose were exposed to SiaPG, under conditions mimicking physiological (pH  
765 7.4 200 mM NaCl). Reactions were quenched by commencing the thiobarbituric acid assay at 1, 2,  
766 and 3 min, and the rate of Neu5Ac release determined by application of a Neu5Ac standard curve.  
767 (A) Michaelis–Menten plot, rate of 4-MU release ( $V_0$ ,  $\mu\text{mol MU released min}^{-1} \text{mg}^{-1} \text{SiaPG}$ ), plotted  
768 against [3- or 6- sialyllactose] ( $\mu\text{M}$ ) using Prism 7 (GraphPad). Error bars = SEM. (B) Table  
769 summarising Michaelis-Menten reaction kinetics and catalytic efficiency of SiaPG and MU-NANA, the  
770 table includes the  $k_{cat}$  (4-MU release  $\text{min}^{-1}$ ), and  $k_{cat}/K_M$  ( $\mu\text{M min}^{-1}$ ). Data shown represent the mean  
771 ( $\pm$  S.D.) of one experiment, where each condition was repeated three times per experiment.

772 **Figure 4. Desialylation of host-relevant glycans by SiaPG.** UHPLC chromatogram showing elution of

773 FA2G2S2 and SLeX with and without digestion by SiaPG. FA2G2S2 contains  $\alpha$ 2-6 linked Neu5Ac.  
774 Some contaminating glycans can be observed in the undigested sample, but these also appear to be  
775 desialylated. Gc = N-glycolylneuraminic acid. SLeX contains  $\alpha$ 2-3 linked Neu5Ac.

776 **Figure 6. Inhibition of periodontal pathogen sialidase activity by zanamivir.** MUNANA was exposed  
777 to periodontal pathogens or purified sialidases. Sialidase activity was expressed as the difference in  
778 4-MU fluorescence relative to conditions with no inhibitor. A) MUNANA was exposed to *T. forsythia*  
779 or *P. gingivalis* in the presence of zanamivir for 1 hour and 4 hours, respectively. Data represent the  
780 mean of two experimental repeats, where each condition was performed three times per  
781 experiment. Error bars = SD. B) MUNANA was exposed to SiaPG and NanH in the presence or  
782 absence of zanamivir (1-10 mM, 1 mM increments), and the IC50 of zanamivir for both enzymes  
783 obtained using the variable slope model in Graphpad Prism 7. Data represent the mean of three  
784 experiments, where each condition was repeated three times. Error bars=SEM.

785 **Figure 7. Enzyme synergy in sialic acid release from BSM, and inhibition by zanamivir.** BSM was  
786 incubated with either NanS, SiaPG, or NanS + SiaPG, in the presence or absence of 0.5 mM  
787 zanamivir, before undergoing the TBA assay to assess sialic acid release. Data based on the mean of  
788 three experiments, each condition was tested in triplicate during each experiment. Error Bars=SEM.  
789 Significance determined by one-way ANOVA with repeated measures, with Bonferroni correction for  
790 multiple comparisons (\*p<0.05, \*\*p<0.01).

791 **Figure 8. Zanamivir inhibits *P. gingivalis* growth and biofilm formation on sialoglycoproteins.**  
792 Bacteria were cultured for 5 days at 37 °C anaerobically, in the presence of Neu5Ac, or on surfaces  
793 coated with the glycoproteins mucin, saliva, or serum. All conditions were performed in the  
794 presence or absence of zanamivir. A) Total growth; OD<sub>600</sub> of the culture was used to quantify  
795 bacteria in both biofilm and planktonic states. B) Biofilm formation, quantified by resuspension of  
796 biofilms and counting the number of bacteria under microscopy. All data shown represent the mean  
797 of three biological repeats, where conditions were tested three times per experiment. Error bars  
798 =SEM. Significance determined by T-test, \*\*p=>0.01, \*\*\*p=>0.005.

799 **Figure 9. Biofilm formation by *P. gingivalis* 381, sialidase deficient Pg381ΔsiaPG, and SiaPG  
800 complemented strain ΔsiaPG<sup>+</sup>.** *P. gingivalis* strains were resuspended to an OD<sub>600</sub> 0.5, and seeded  
801 into microtitre plates precoated with mucin (BSM), and biofilms were cultured for 24 hours at 37°C  
802 anaerobically. Data represent the mean of four replicates per condition. Error bars = SD, statistical  
803 significance determined by unpaired T-test compared to the WT strain, \*\*p=<0.01).

804 **Figure 10. Purified sialidases desialylate oral epithelial cell surfaces, and in the case of SiaPG this is  
805 inhibited by zanamivir.** Cells were stained with lectins for α2-3 and α2-6 linked sialic acid in red and  
806 green, respectively. Prior to staining, cells were treated with NanH and SiaPG in PBS, in the presence  
807 or absence of 10 mM zanamivir (zan), as indicated. All images were visualised using the same

808 microscopy and image processing parameters (fluorescence intensity, exposure time and  
809 background subtraction). Images were captured in three fields of view, and this was repeated in  
810 three separate experiments. Images shown are representative of each condition. Separate colour  
811 channels are displayed in the supplementary information (supplemental figure S3).

812 **Figure 11. The effect of zanamivir on attachment and invasion of epithelial cells during**  
813 **monospecies infection.** Antibiotic protection assays on OKF6 and H357 cell lines were performed in  
814 the presence or absence of 10 mM zanamivir (thatched and black bars, respectively) with either A) *T.*  
815 *forsythia*, B) *P. gingivalis*, or C) *F. nucleatum*. Bacterial attachment, invasion, and total association  
816 with host cells was normalised to the number of bacteria that were used to infect each condition  
817 that had survived the duration of the assay (the percentage of viable bacteria). Data represent the  
818 mean from three independent experimental repeats, and each condition was repeated in triplicate  
819 during each experiment. Error bars=SEM, Significance determined by paired T-test, \* $p < 0.05$ , \*\*

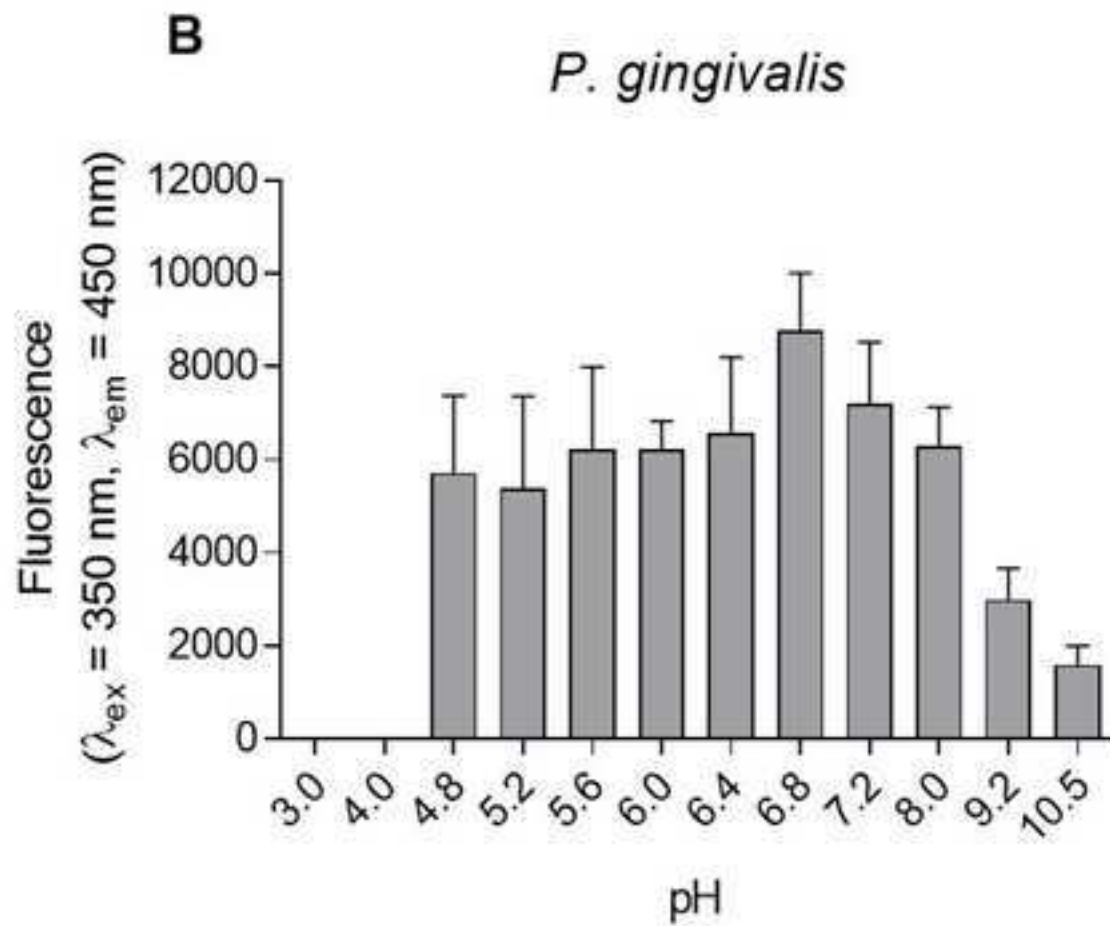
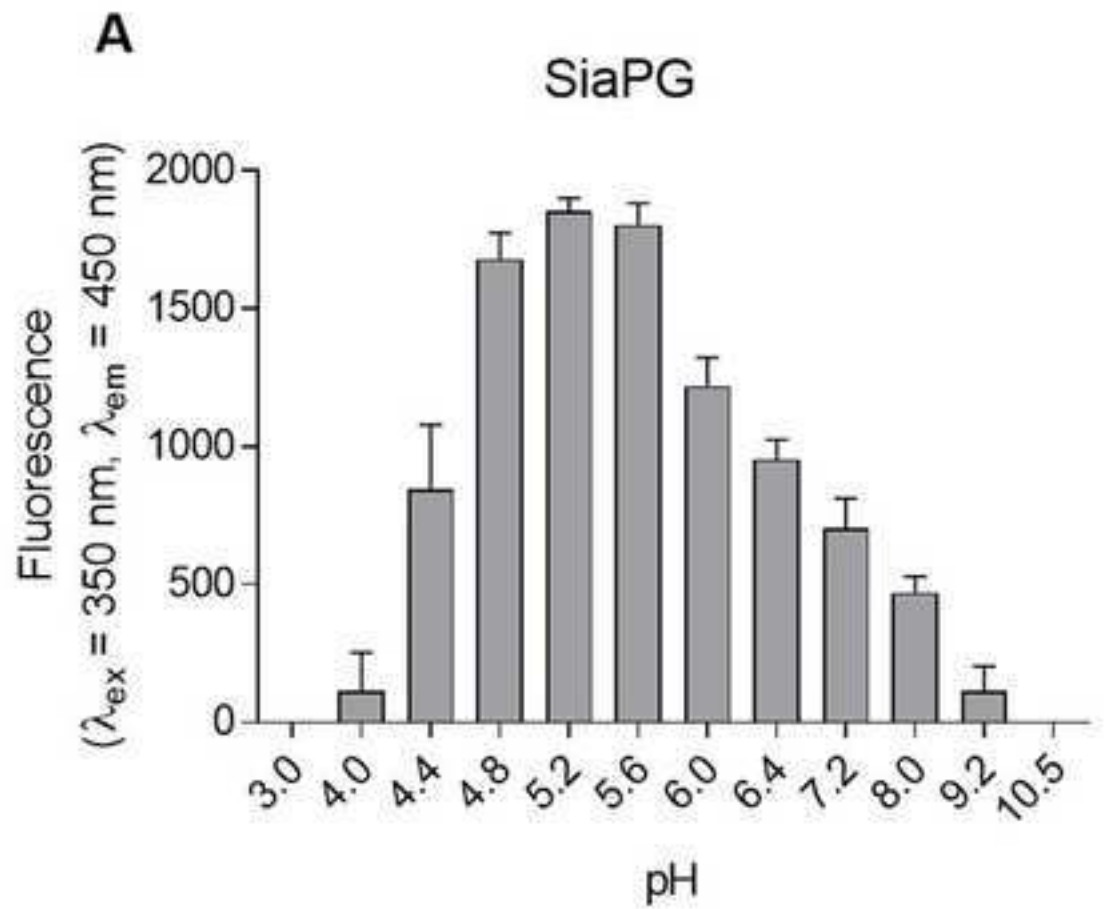
820 **Figure 12. The effect of zanamivir on attachment and invasion of epithelial cells during**  
821 **multispecies infection.** Antibiotic protection assays were performed in the presence or absence of  
822 10 mM zanamivir (thatched and black bars, respectively) with different combinations of *T. forsythia*,  
823 *F. nucleatum*, and *P. gingivalis* to establish host cell association in each instance. A) *T. forsythia* + *F.*  
824 *nucleatum* B) *T. forsythia* + *P. gingivalis*. C) *F. nucleatum* + *P. gingivalis* D) *T. forsythia*, *F. nucleatum*,  
825 and *P. gingivalis*. Bacterial attachment, invasion, and total association with host cells was normalised  
826 to the number of bacteria that were used to infect each condition that had survived the duration of  
827 the assay (the percentage of viable bacteria). Zanamivir = 10 mM zanamivir present during host cell  
828 exposure to bacteria. Data represent the mean from three experimental repeats, and each condition  
829 was repeated in triplicate during each experiment. Error bars=SEM, Significance determined by  
830 paired T-test, \* $p < 0.05$ , \*\* $p < 0.01$ . \*\*\* $p < 0.001$ .

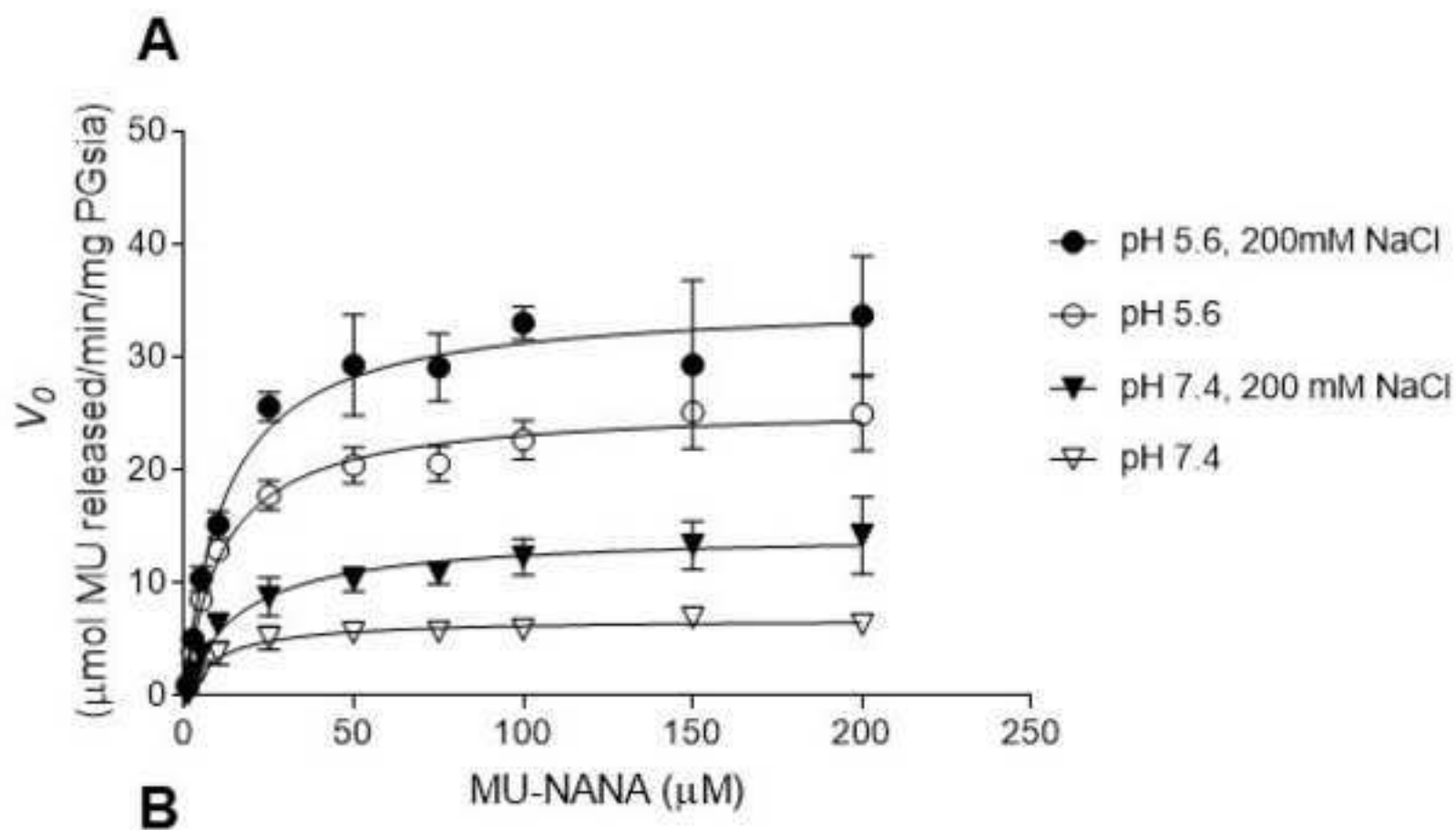
831 **Table 1. List of primers used in this study**

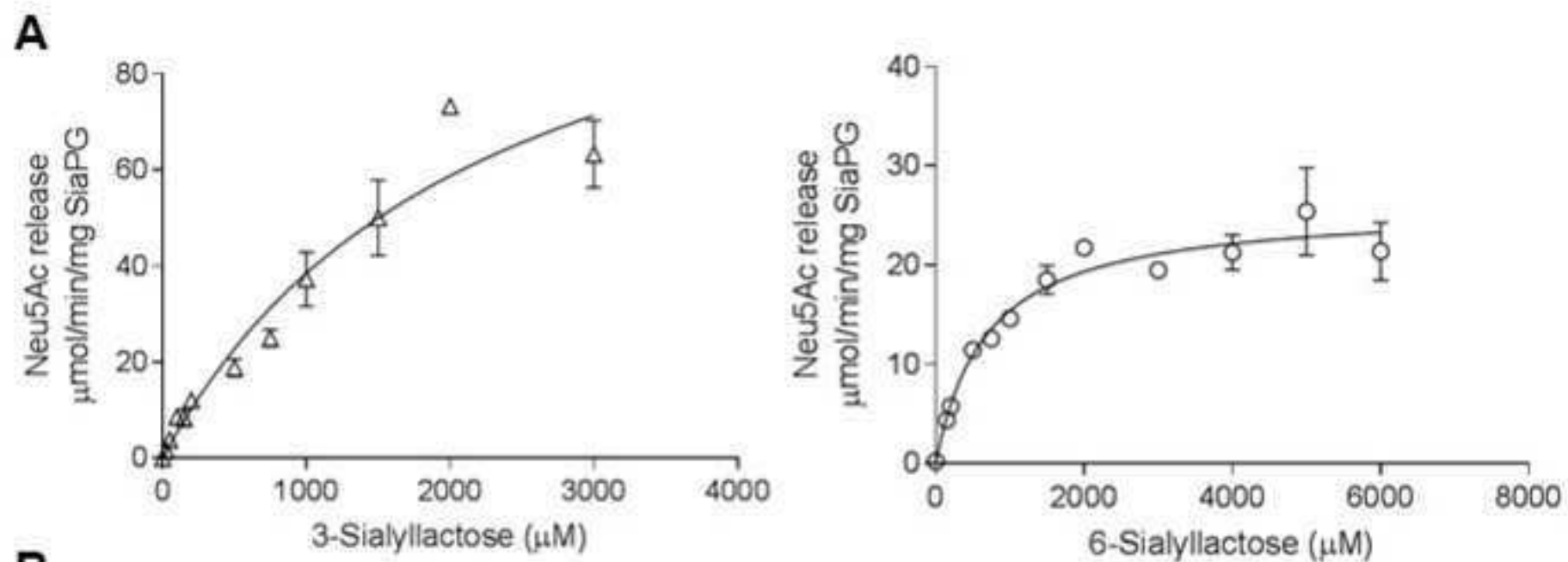
832

Primers for <i>siaPG</i> deletion mutant	
Primer	Sequence (5'>3')
#1	TACGGCATCGCGGTTTTGA
#2	TCGCCATAGAATACAGGATAAGC
#3	gggcaatttctttttgtcatTGAAAAC TATTTTATACCATTTTGGGA
#4	TCCAAAATGGTATAAAATAGTTTCAatgacaaaaaagaaattgcc
#5	aaaaatttcaccttcgtagGAATAGTGCTTTTTTATCGAGTTTTTC
#6	GAAAAACTCGATAAAAAAAGCACTATT Cctacgaaggatgaaat
Sequences in upper case correspond to <i>siaPG</i> and lower case to <i>ermF</i> .	
Primers for <i>siaPG</i> complementation	
FWD BamHI	<u>CGCGGATCCG</u> taatagactcactatagg
REV Sall	TTGAC <u>GTCGACG</u> CTtagttattgctcagcgggtgg
Endonuclease sites are underlined.	

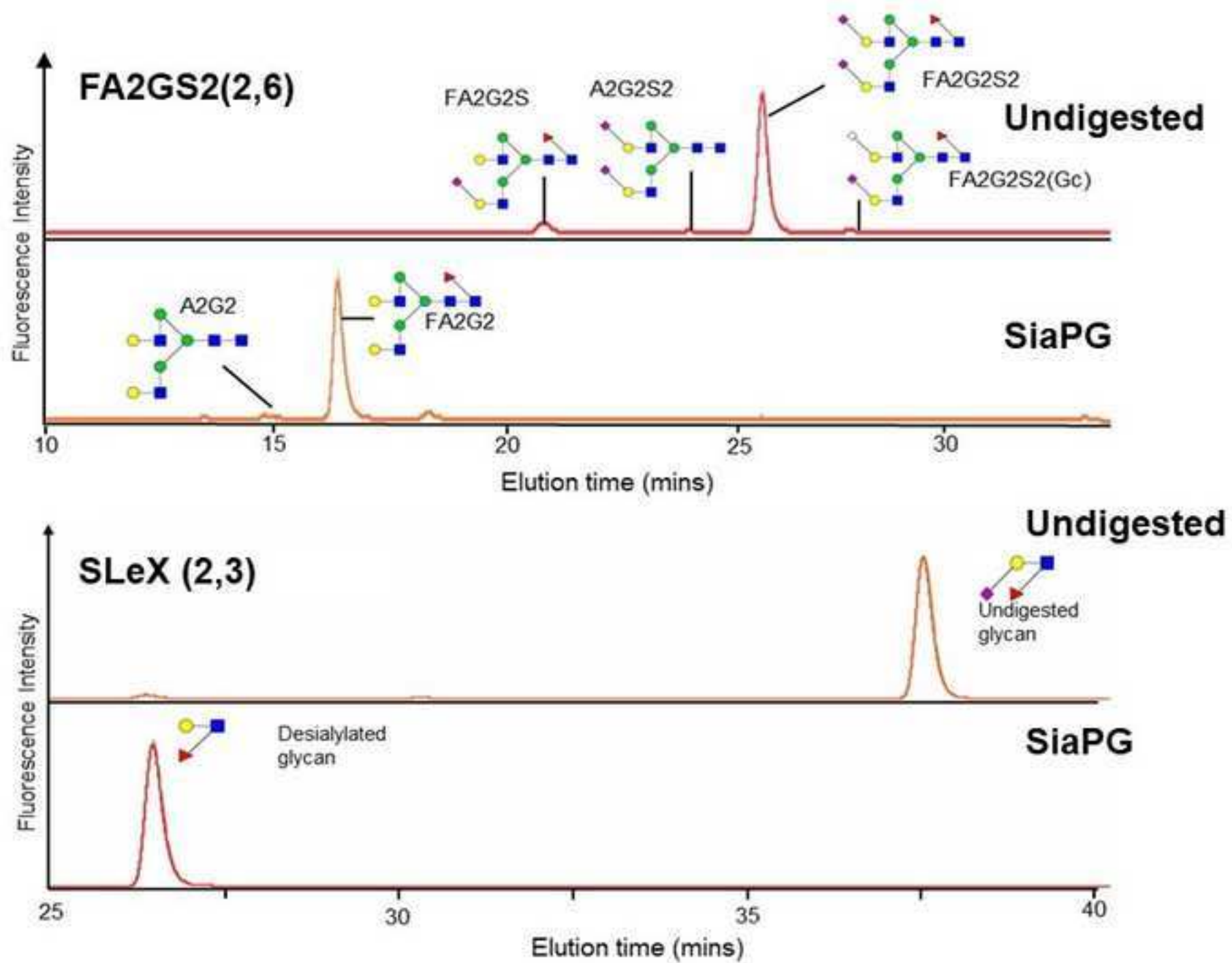
833

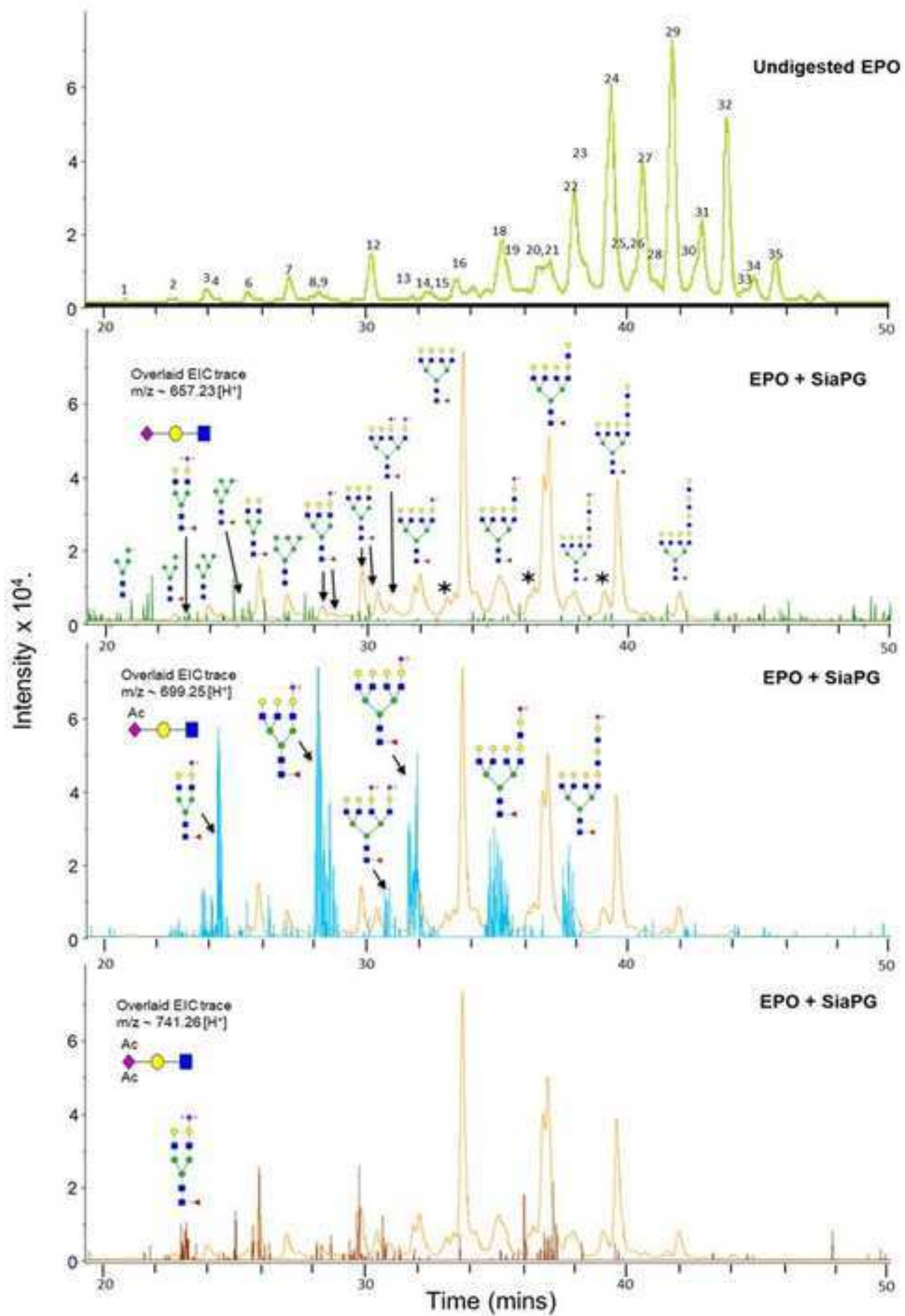


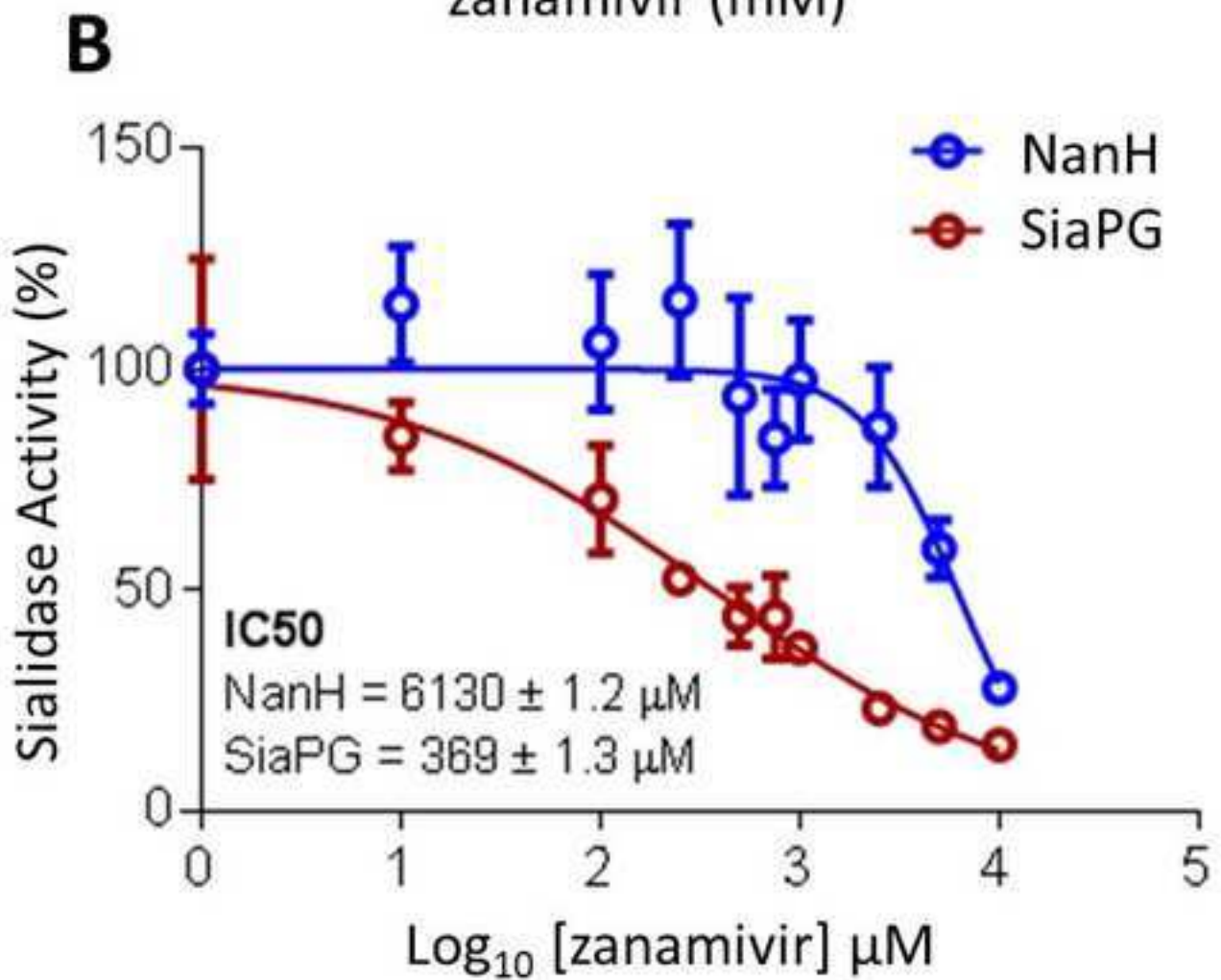
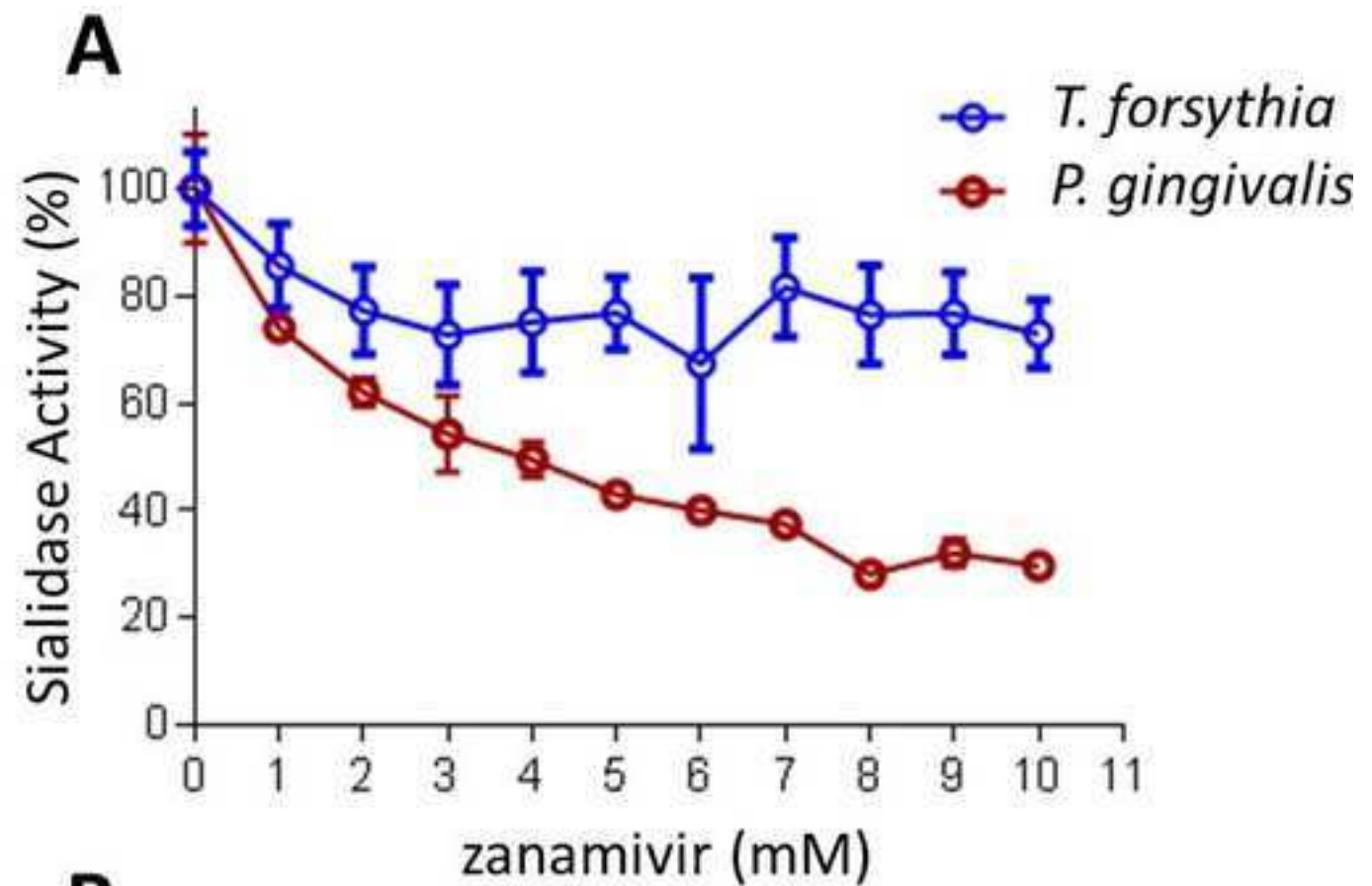


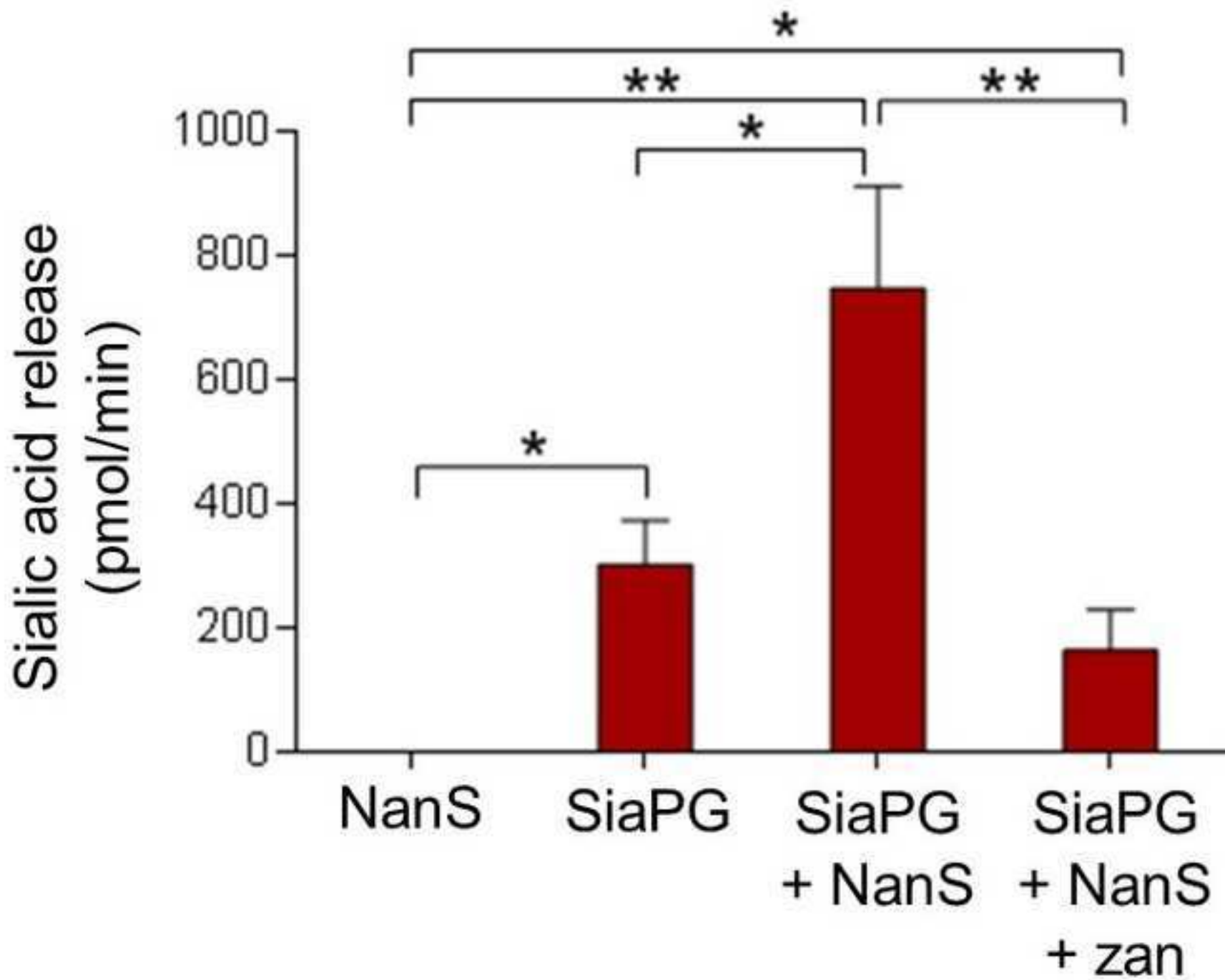
**B**

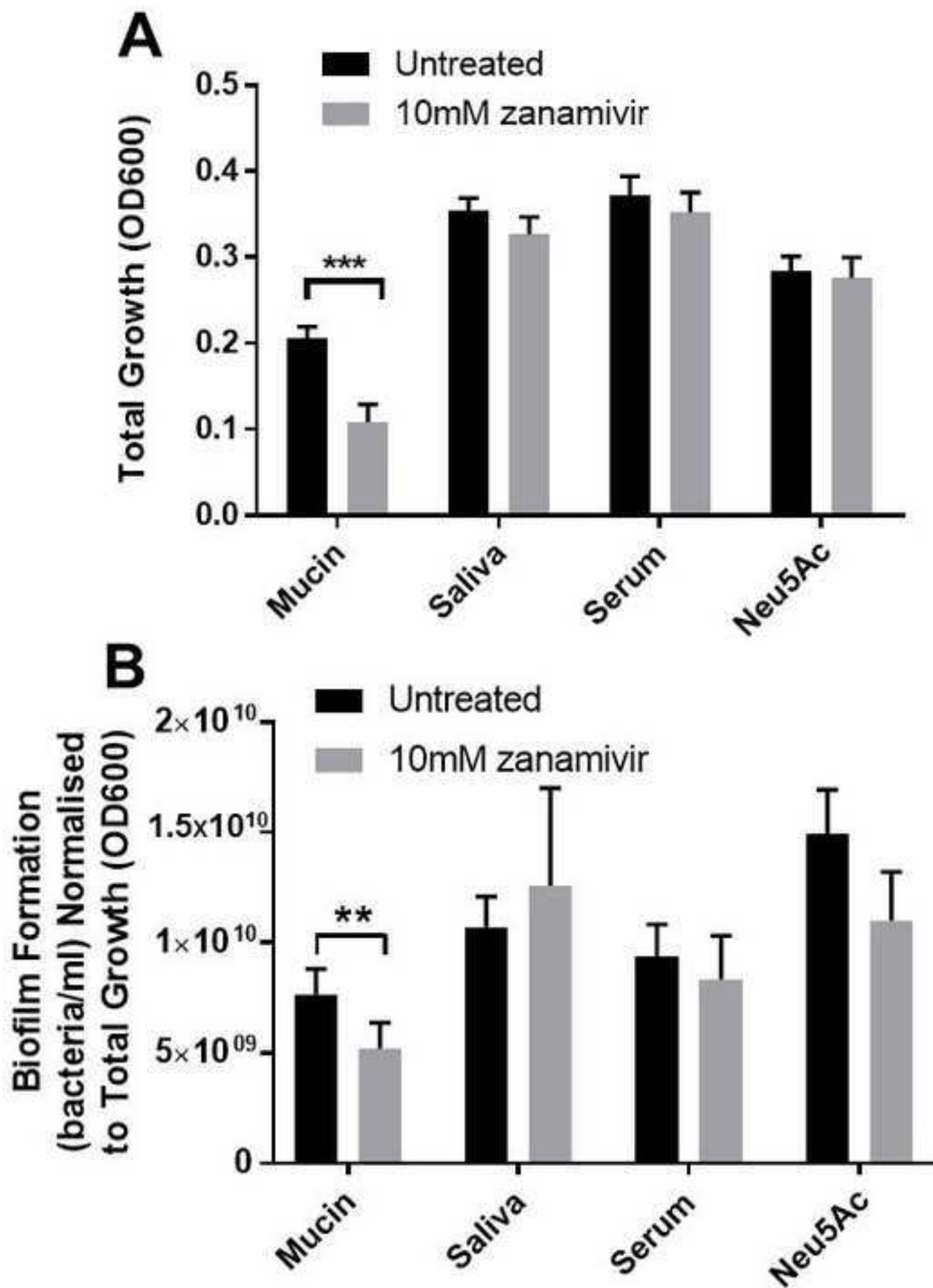
	3-Sialyllactose	6-Sialyllactose
$K_{cat}$ (Neu5Ac release/min)	$356.8 \pm 49.64$	$74.42 \pm 2.8$
$K_M$ ([Sialyllactose], $\mu\text{M}$ )	$2234 \pm 548.8$	$684.9 \pm 92.6$
$K_{cat}/K_M$ ( $\mu\text{M}/\text{min}$ )	0.16	0.11
$V_{max}$ (Neu5Ac release, $\mu\text{mol}/\text{min}/\text{mg}$ SiaPG)	$124.3 \pm 17.3$	$25.9 \pm 1.0$

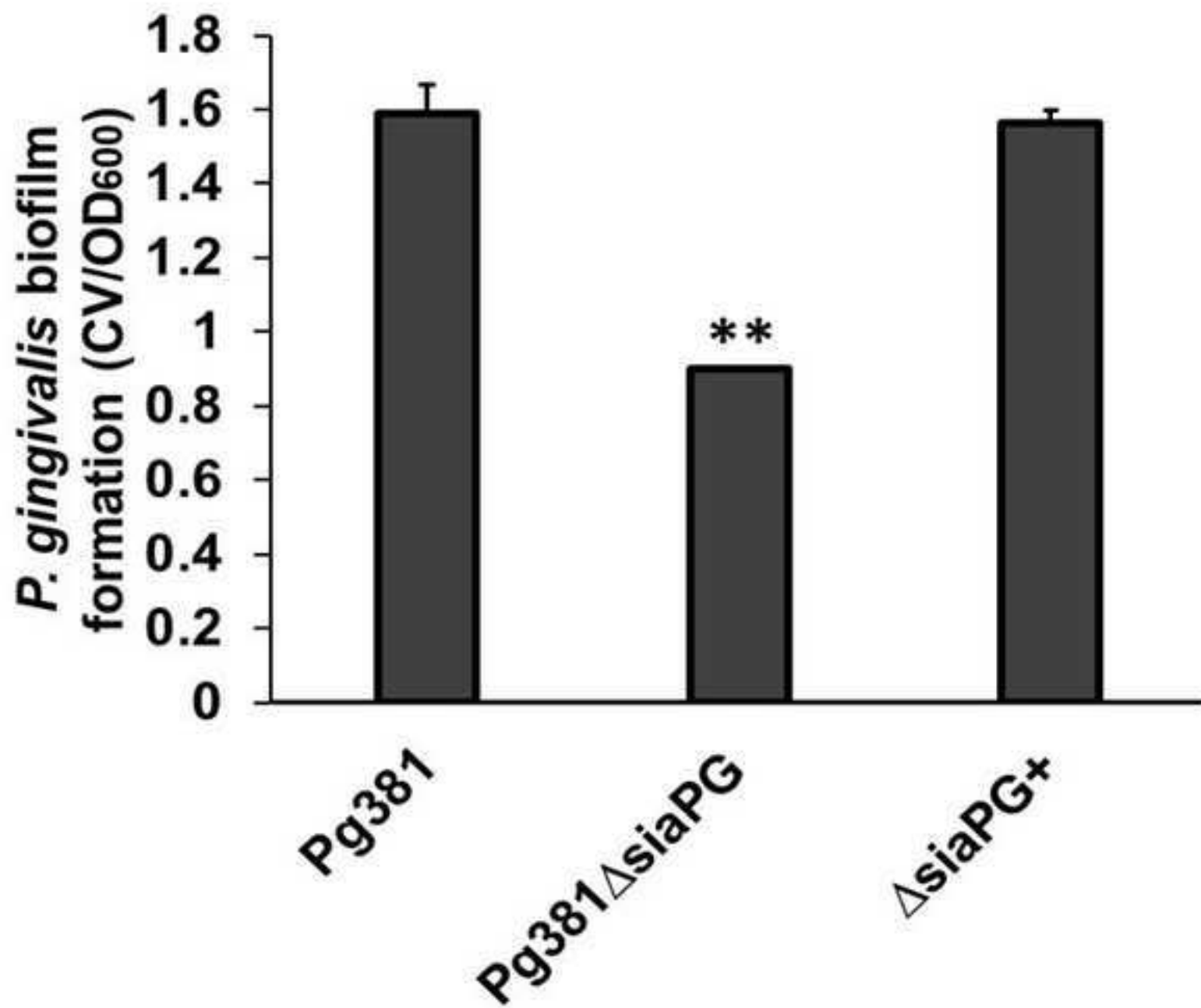


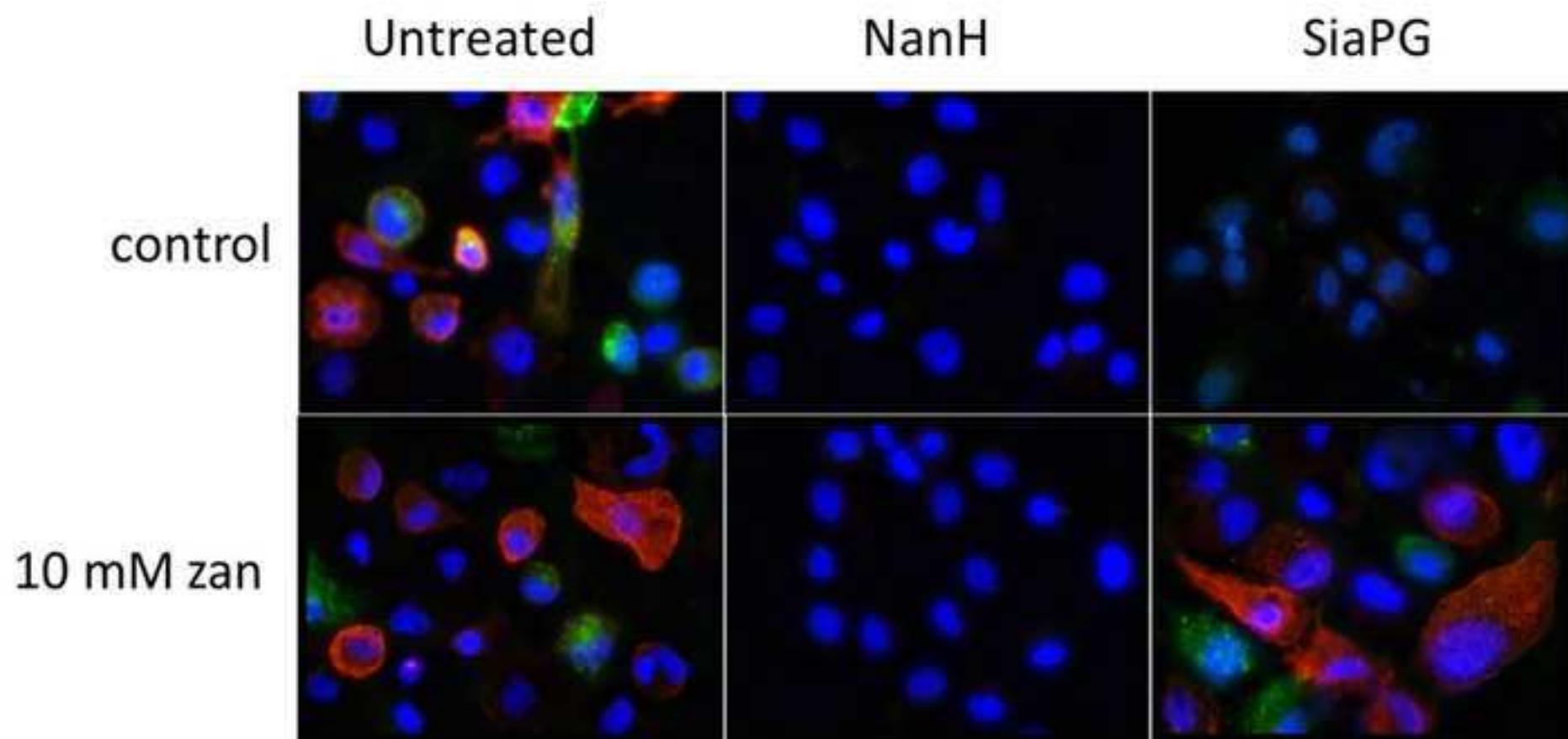


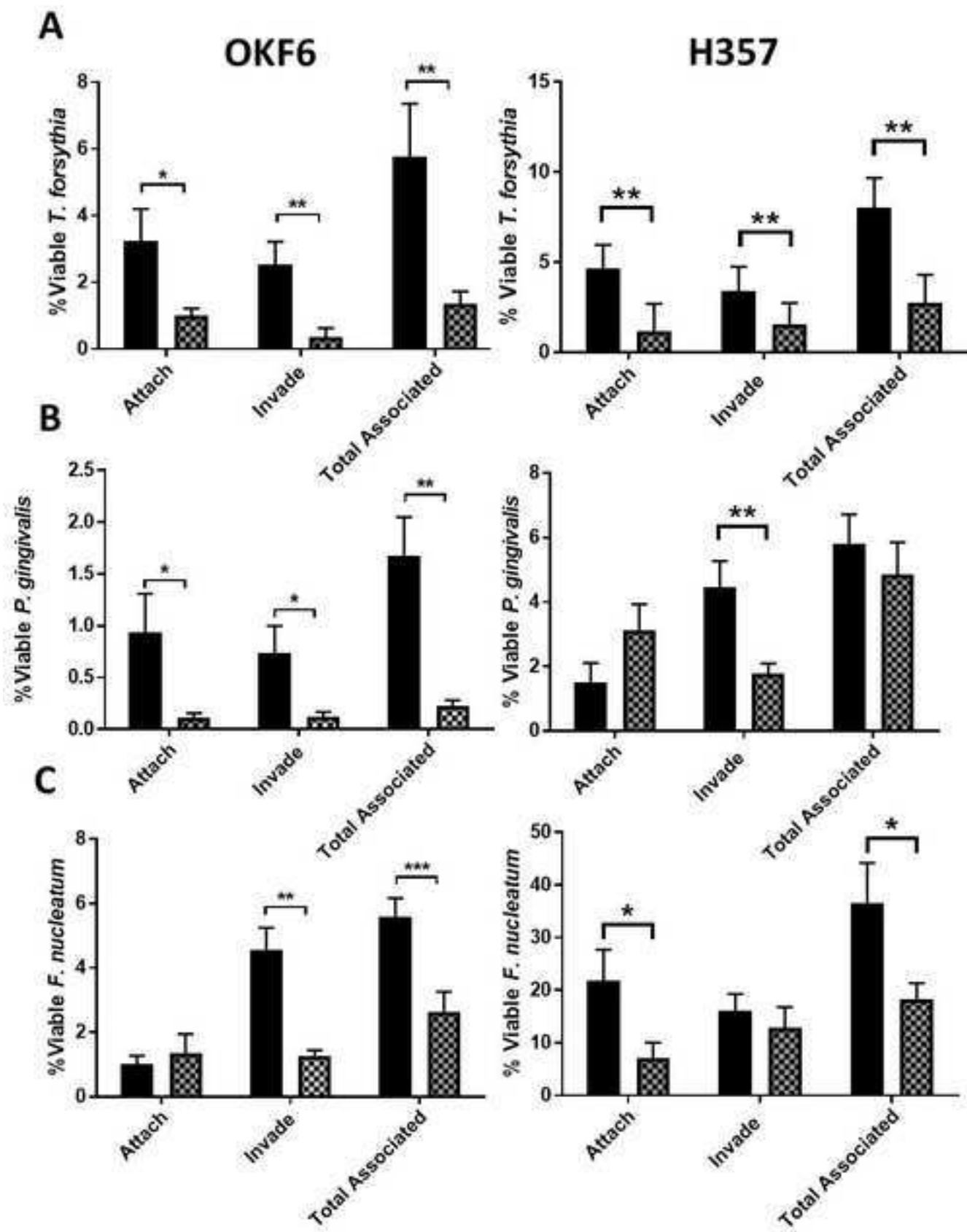


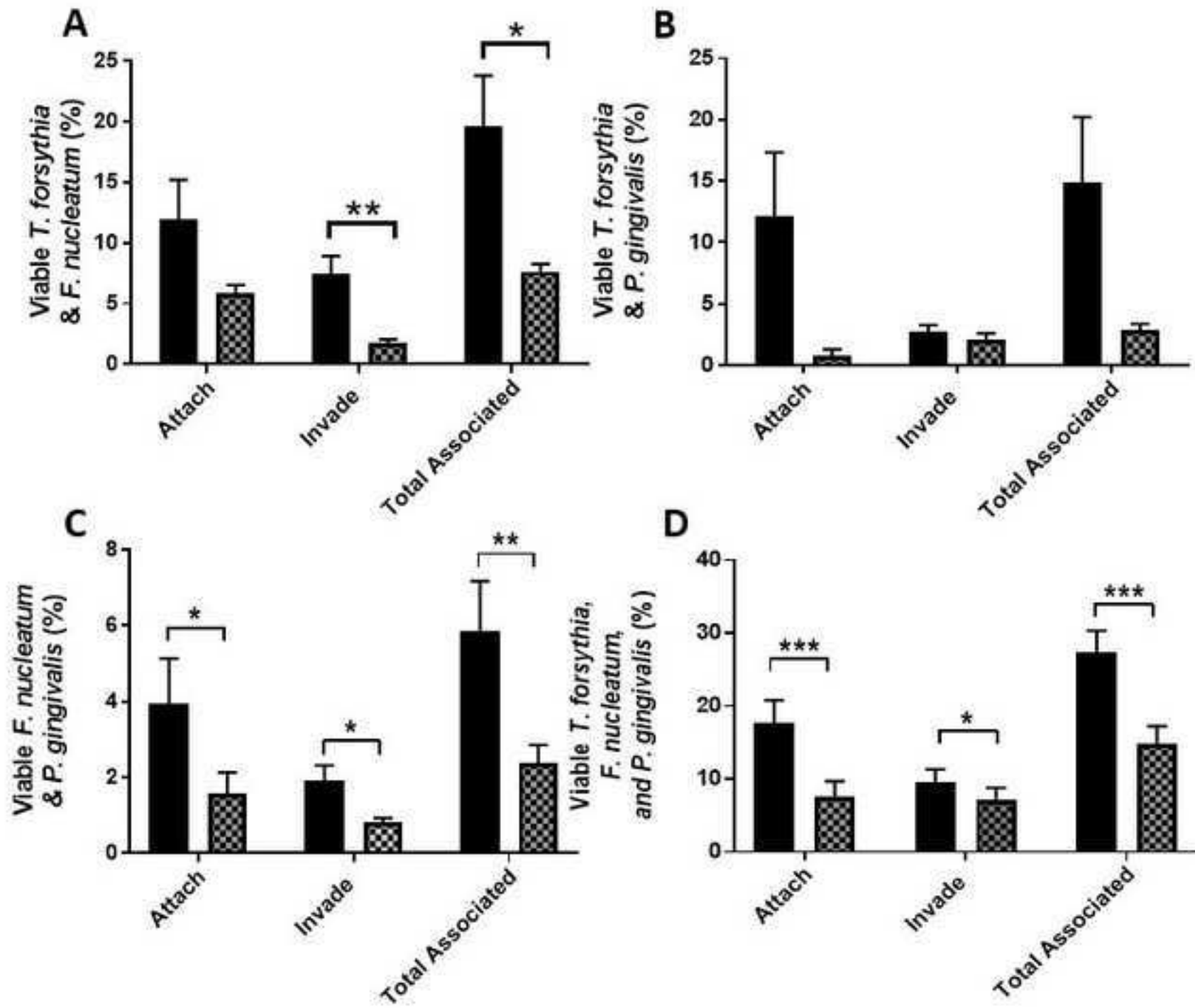


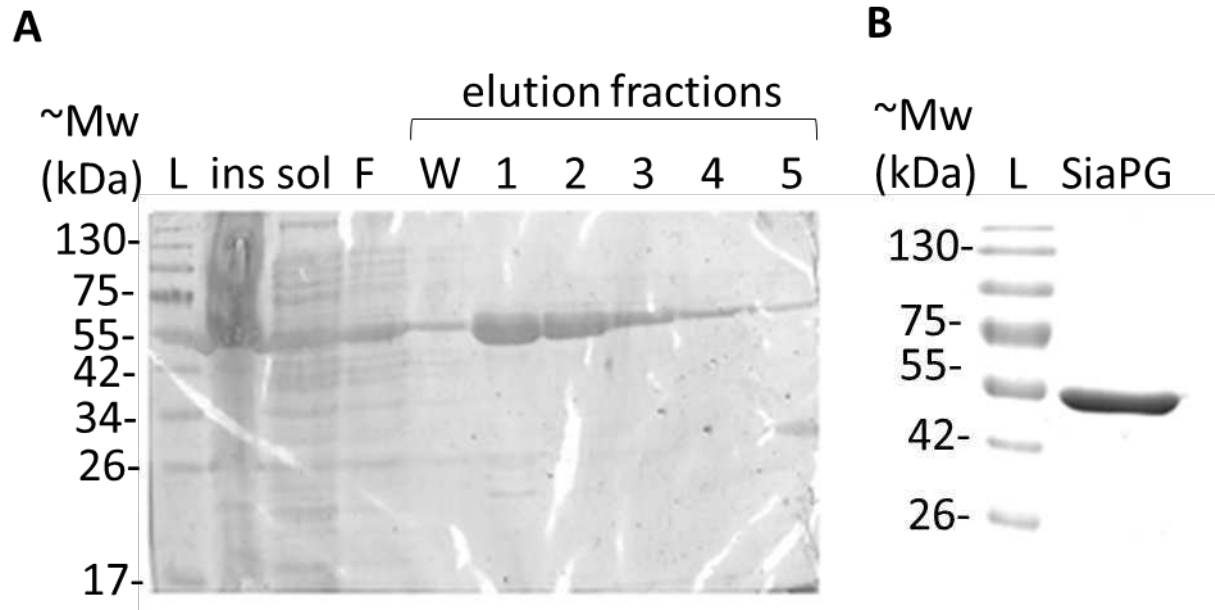








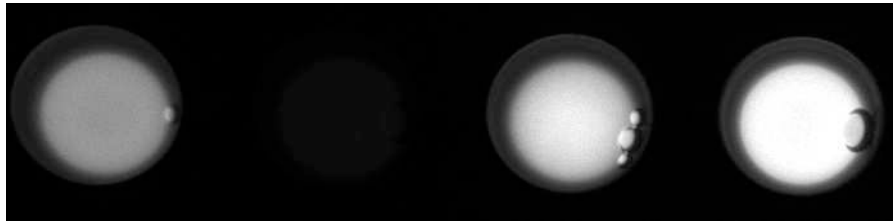


**C**

Native protein

MANNTLLAKTRRYVCLVVFCCLMAMMHLSGQEVMTMWGDSHGVA PNQVRRTL VKVALSESLPPGAKQIRIGFSLP  
 KETEEKVTALYLLVSDSLAVRDLDPDYKGRVSYDSFPISKEDRTTALSADSVAGRCFFYLAADIGPVASFSDTLTARVE  
 ELAVDGRPLPLKELSPASRRLYREYEALFVPGDGGSRNYRIPSILKTANGTLIAMADRRKYNQTDLPEDIDIVMRRST  
 DGGKSWSDPRIIVQGEGRNHGFGDVALVQTQAGKLLMIFVGGVGLWQSTPDRPQRTYISESRDEGLTWSPPRDI  
 THFIFGKDCADPGRSRWLASFASGQGLVLPGRV MFVAAIRESGQEYVLNNYVLYSDDEGGTWQLSDCAYHRG  
 DEAKLSLMPDGRVLM SVRNQGRQESRQRFFALSSDDGLTWERAKQFEGIHDPGCNGAMLQVKNRGRNQMLHS  
 LPLGPDGRRRDGAVYLFDHVSGRWSAPVVVNSGSSAYSMDMTLLADGTIGYFVEEDDEISLVFIRFVLDDLDFDARQ

**Supplemental figure S1. Purification of SiaPG** A) SiaPG purification via affinity chromatography. L= Molecular mass ladder, ins = insoluble fraction of whole bacterial lysate, sol = soluble fraction of whole bacterial lysate, F = flow through, W = wash, elution fractions were 1 ml each. B) Purified SiaPG post-dialysis. C) Native gene encoding SiaPG and resulting encoded protein (PG\_0352, obtained from UniProt; Q7MX62), 100 % protein identity between W83 and ATCC 33277 strains). Red = secretion signal site, absent in the codon optimized protein expressed here using *E. coli*.



Pg381

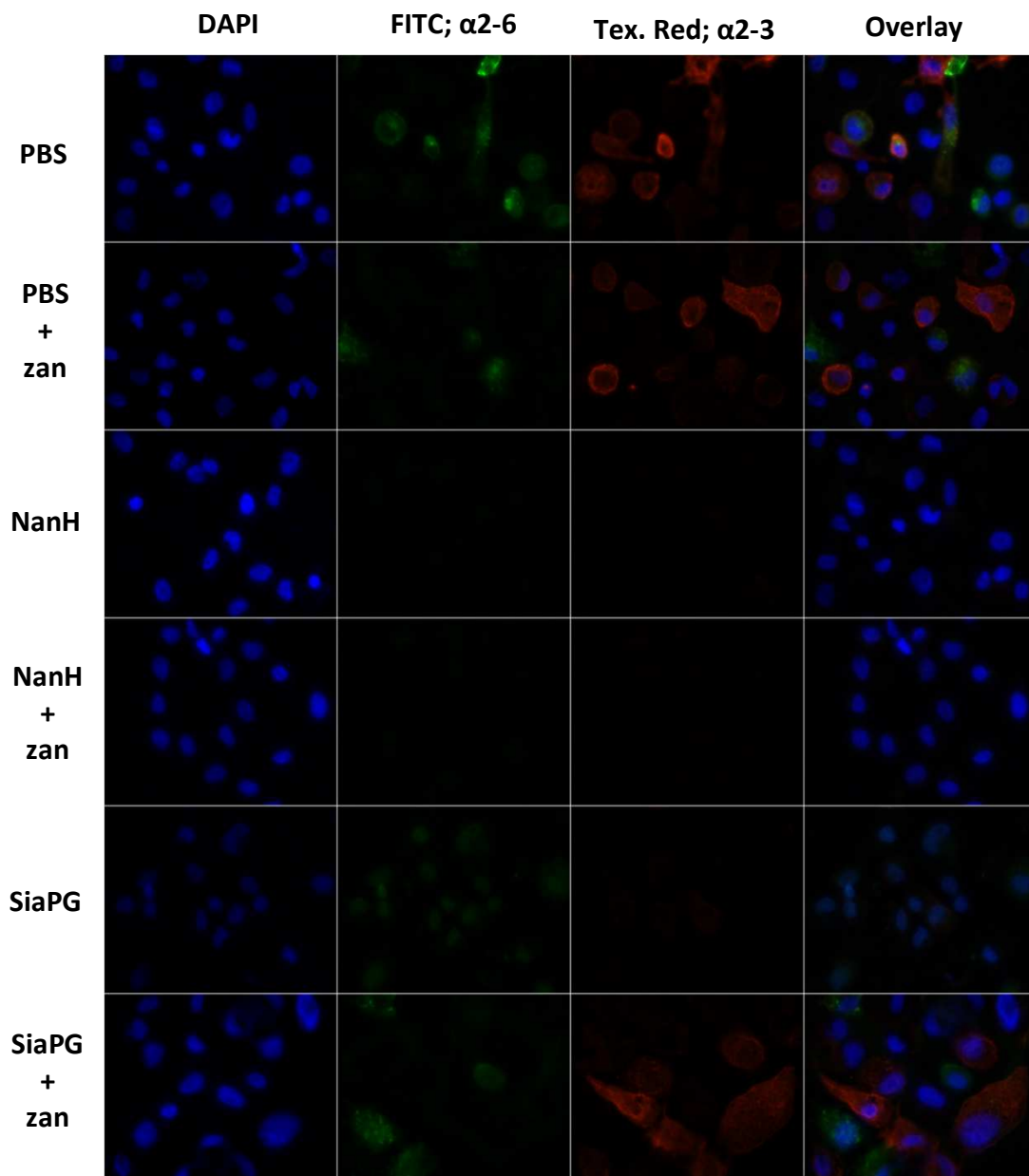
Pg381

SiaPG

$\Delta$ siaPG<sup>+</sup>

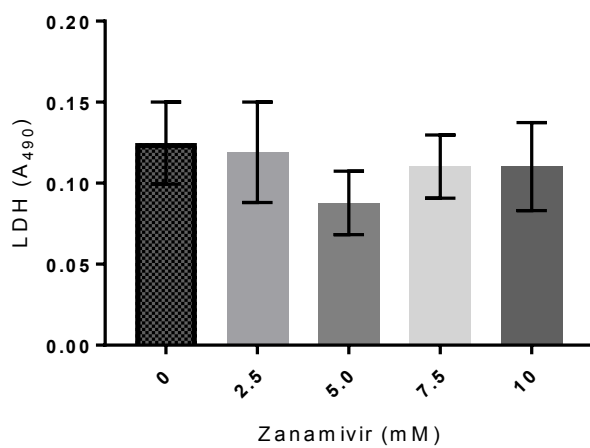
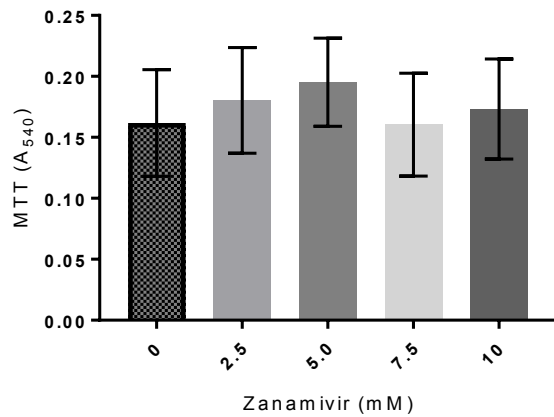
$\Delta$ siaPG

Supplemental figure S2: Sialidase activity of SiaPG, *P. gingivalis* SiaPG-inactivated isogenic mutant (Pg381 $\Delta$ siaPG) and its complemented strain ( $\Delta$ siaPG<sup>+</sup>)



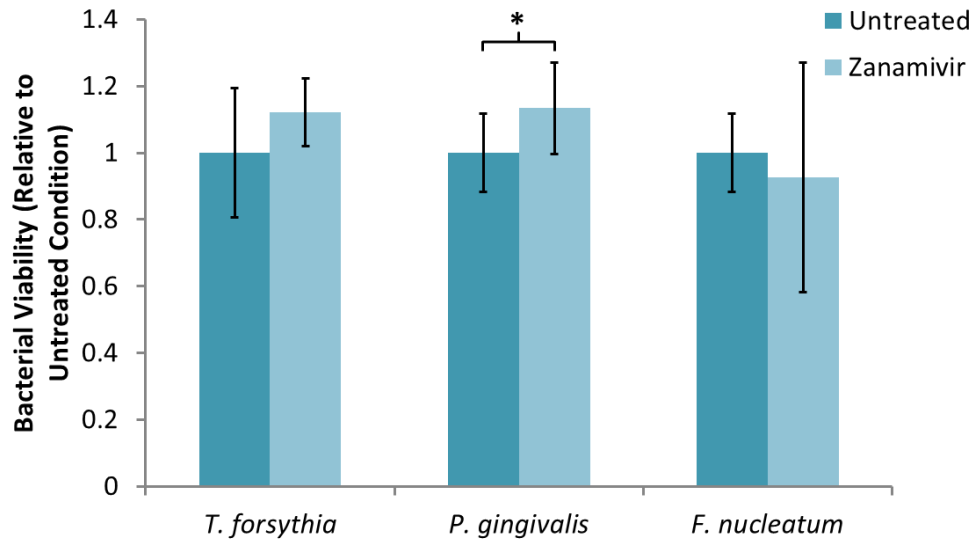
**Supplemental figure S3. Purified sialidases desialylate oral epithelial cell surfaces.**

Cells were stained with lectins for  $\alpha$ 2-3 and  $\alpha$ 2-6 linked sialic acid in red and green, respectively. Prior to staining, cells were treated with NanH and SiaPG in PBS, in the presence or absence of 10mM zanamivir, as indicated. All images were visualised using the same microscopy and image processing parameters (fluorescence intensity, exposure time and background subtraction). Images were captured in three fields of view, and this was repeated in three separate experiments. Images shown are representative of each condition.



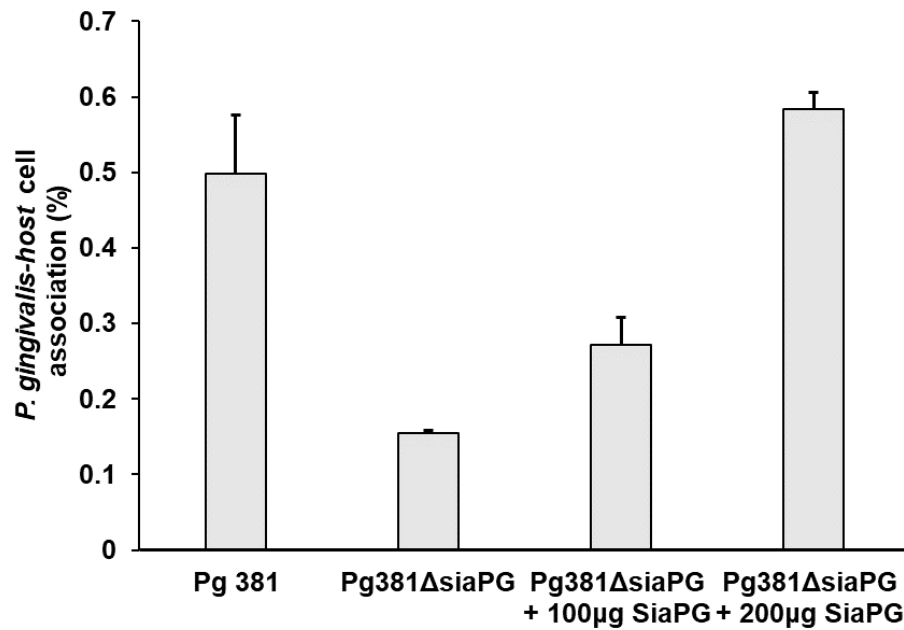
**Supplemental figure S4. Viability testing of OKF6 oral epithelial cells exposed to zanamivir.**

The oral epithelial cell line OKF6 was exposed to *T. forsythia* in the presence and absence of 10 mM zanamivir for 2.5 hours, followed by an MTT assay on cells, or an LDH assay on culture supernatant, with the absorbance at 490 and 540 nm for LDH and MTT, respectively, used to relatively quantify levels of MTT and LDH. Data shown represent the mean of two experiments, where each condition was repeated three times per experiment. Error bars=SEM. No significant differences were found (where  $p < 0.05$ ), as determined by one way ANOVA, with repeated measures and Tukey's correction for multiple comparisons.

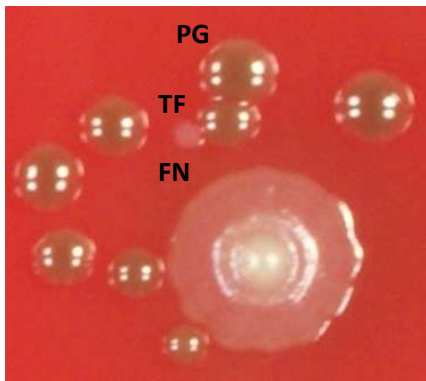


**Supplemental figure S5. Viability testing of periodontal pathogens exposed to zanamivir.**

*T. forsythia*, *P. gingivalis*, and *F. nucleatum* were incubated in the presence and absence of 10mM zanamivir for 2.5 hours, followed by enumeration of viable organisms by agar plate counts, and data were expressed as the change in cell numbers relative to the untreated condition. Data shown represent the mean of three experiments, where each condition was repeated three times per experiment. Error bars=SD. Significance determined by T-test (\*p<0.05).

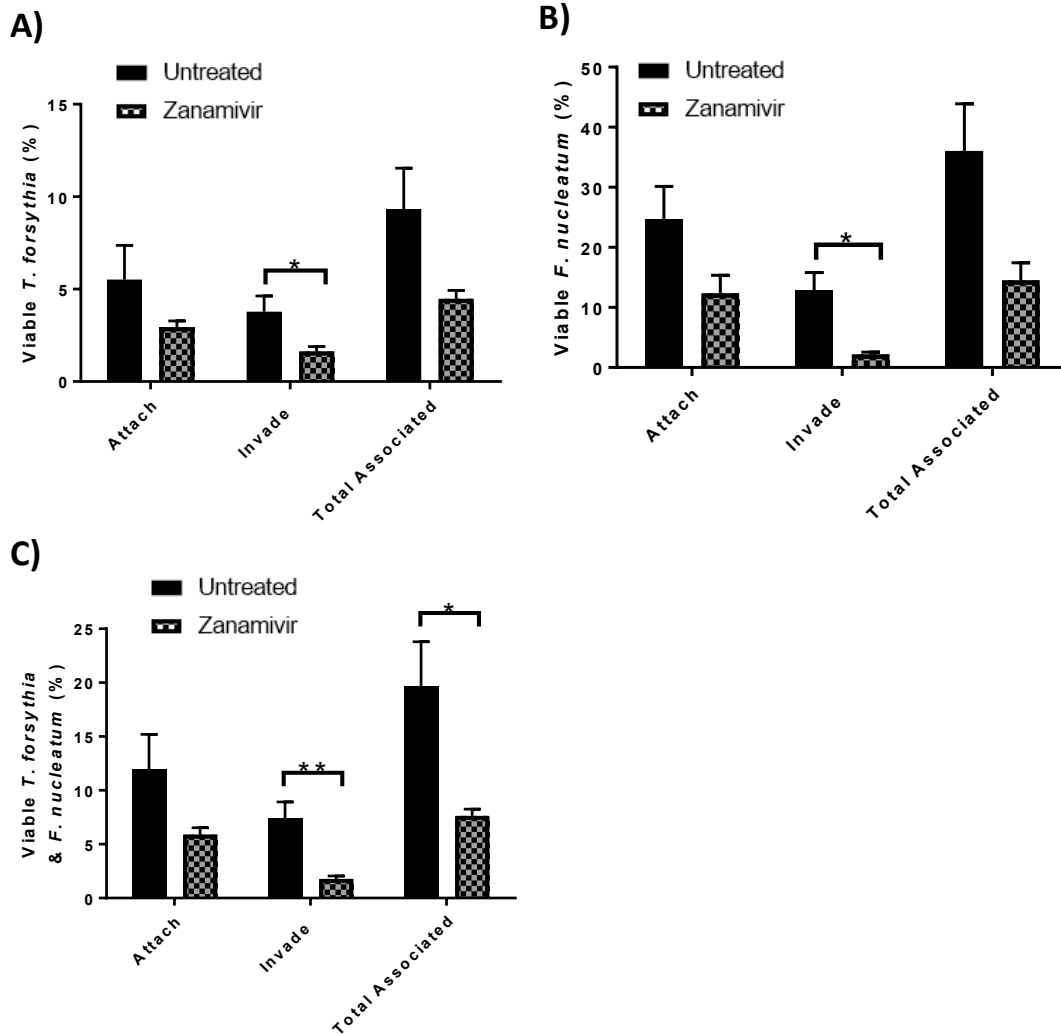


**Supplemental Figure S6. Association of *P. gingivalis* with OBA9 cells.** OBA-9 cells were incubated with *P. gingivalis* 381 or the SiaPG inactivated mutant ( $\Delta$ PG352), in the presence or absence of 100 and 200  $\mu$ g of SiaPG. Bacterial association was calculated as percentage of input bacteria. Data represent the mean of two experiments, where each condition was repeated three times per experiment. Error bars = SEM, significant differences between Pg 381 and the other conditions were determined by paired T-test, \* $p$ <0.05, \*\* $p$ <0.01).



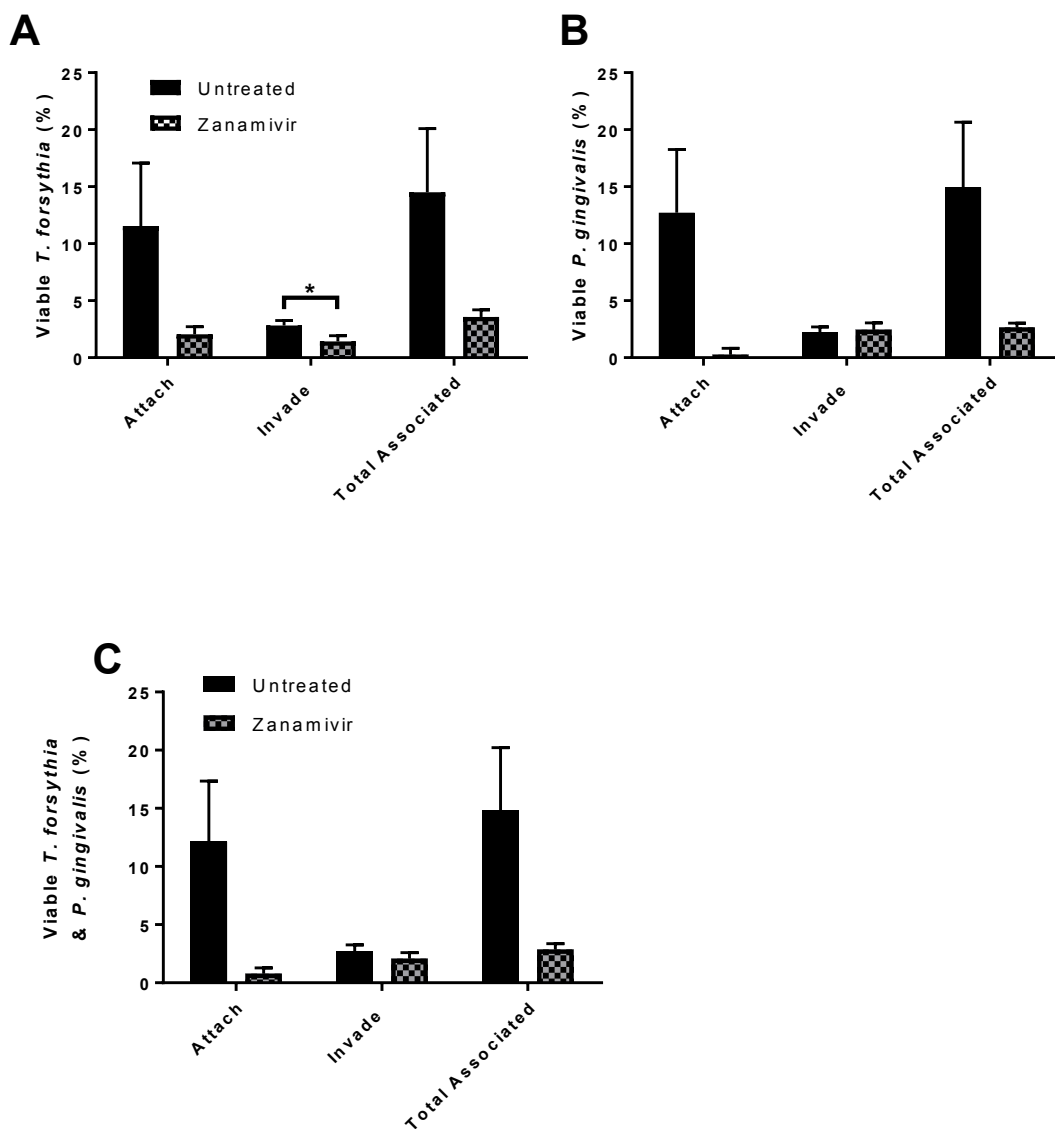
**Supplemental figure S7. Colony morphology of *P. gingivalis*, *F. nucleatum*, and *T. forsythia* during mixed-species enumeration.**

Images of mixed-species agar cultures to highlight differences in colony morphology. Left panel = unassisted view, right panel = colony counter microscope view. One colony representative of each species is labelled on the images. *P. gingivalis* (PG) forms opaque black-pigmented colonies, *T. forsythia* (TF) forms translucent grey colonies, and *F. nucleatum* (FN) forms large beige colonies, translucent at the edges with a raised, opaque centre.



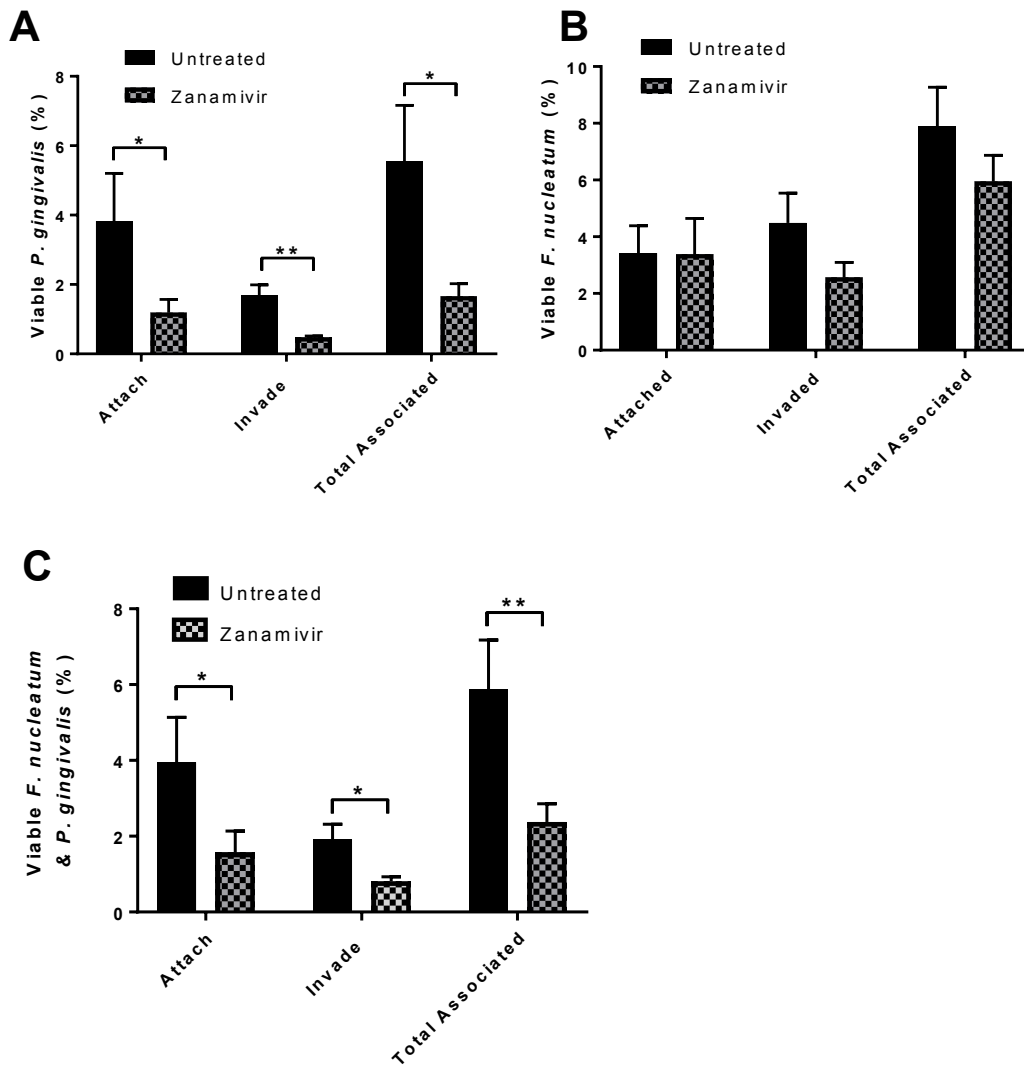
**Supplemental figure S8. The effect of zanamivir on attachment and invasion of epithelial cells co-infected with *T. forsythia* and *F. nucleatum*.**

Antibiotic protection assays were performed in the presence or absence of zanamivir with *T. forsythia* and *F. nucleatum*. A) Level of *T. forsythia*-host cell association, B) Level of *F. nucleatum*-host cell association, or C) Level of both *T. forsythia* and *F. nucleatum*-host cell association. Bacterial attachment, invasion, and total association with host cells was normalised to the number of bacteria that were used to infect each condition that had survived the duration of the assay (the percentage of viable bacteria). Zanamivir= 10mM zanamivir present during host cell exposure to bacteria. Data represent the mean from three experimental repeats, and each condition was repeated in triplicate during each experiment. Error bars=SEM, Significance determined by paired T-test, \* $p < 0.05$ , \*\* $p < 0.01$ .



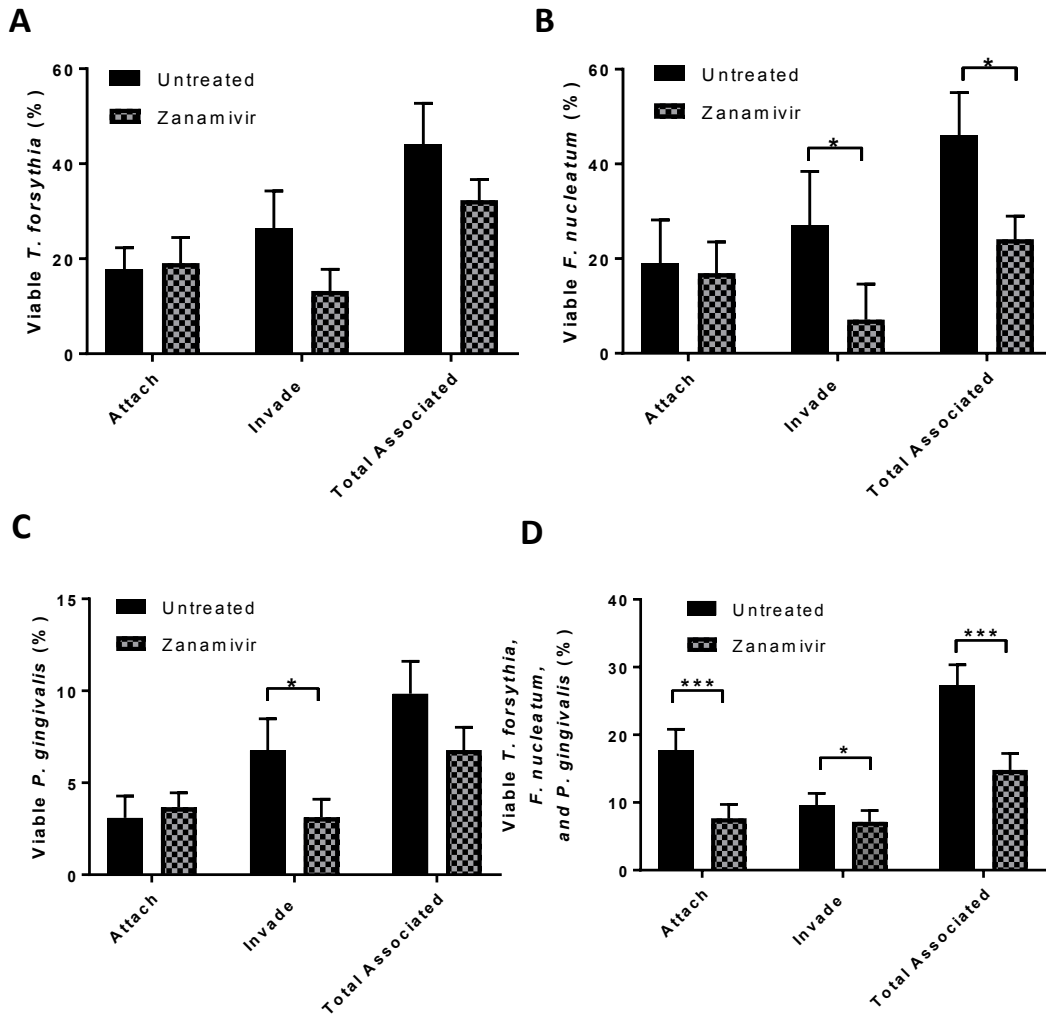
**Supplemental figure S9. The effect of zanamivir on attachment and invasion of epithelial cells co-infected with *T. forsythia* and *P. gingivalis*.**

Antibiotic protection assays were performed in the presence or absence of zanamivir with *T. forsythia* and *P. gingivalis* A) Level of *T. forsythia*-host cell association, B) Level of *P. gingivalis*-host cell association, or C) Level of both *T. forsythia* and *P. gingivalis*-host cell association. Bacterial attachment, invasion, and total association with host cells was normalised to the number of bacteria that were used to infect each condition that had survived the duration of the assay (the percentage of viable bacteria). Zanamivir= 10 mM zanamivir present during host cell exposure to bacteria. Data represent the mean from three experimental repeats, and each condition was repeated in triplicate during each experiment. Error bars=SEM. Significance determined by paired T-test, \* $p < 0.05$ .



**Supplemental figure S10. The Effect of Zanamivir on Attachment and Invasion of Epithelial Cells Co-infected with *P. gingivalis* and *F. nucleatum*.**


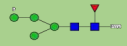
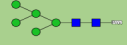

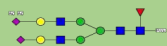
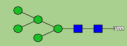








Antibiotic protection assays were performed in the presence or absence of zanamivir with *T. forsythia* and *F. nucleatum* A) Level of *T. forsythia*-host cell association, B) Level of *F. nucleatum*-host cell association, or C) Level of both *P. gingivalis* and *F. nucleatum*-host cell association. Bacterial attachment, invasion, and total association with host cells was normalised to the number of bacteria that were used to infect each condition that had survived the duration of the assay (the percentage of viable bacteria). Zanamivir=10mM zanamivir present during host cell exposure to bacteria. Data represent the mean from three experimental repeats, and each condition was repeated in triplicate during each experiment. Error bars=SEM, Significance determined by paired T-test, \* $p < 0.05$ , \*\* $p < 0.01$ .



**Supplemental figure S11. The effect of zanamivir on attachment and invasion of epithelial cells co-infected with *T. forsythia*, *F. nucleatum*, and *P. gingivalis*.**

Antibiotic protection assays were performed in the presence or absence of zanamivir with *T. forsythia*, *F. nucleatum*, and *P. gingivalis*. A) *T. forsythia*-host cell association, B) *F. nucleatum*-host cell association, C) *P. gingivalis*-host cell association D) *T. forsythia*, *F. nucleatum*, and *P. gingivalis*-host cell association. Bacterial attachment, invasion, and total association with host cells was normalised to the number of bacteria that were used to infect each condition that had survived the duration of the assay (the percentage of viable bacteria). Zanamivir=10mM zanamivir present during host cell exposure to bacteria. Data represent the mean from three experimental repeats, and each condition was repeated in triplicate during each experiment. Error bars=SEM, Significance determined by paired T-test, \* $p < 0.05$ , \*\* $p < 0.01$ . \*\*\* $p < 0.001$ .

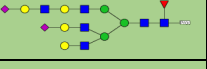
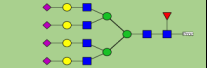
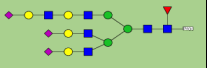
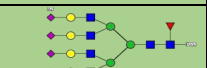
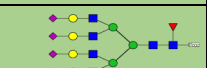
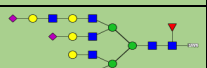
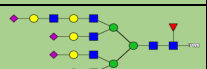
Supplemental table 1. Composition of EPO glycans.



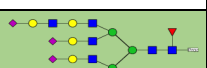

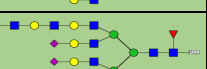



UHPLC Peak ID	% Area	ESI-LC/MS								
		Composition								
		Possible structure	Example Glycan cartoon	Hex (H)	HexNAc (N)	Fuc (F)	Neu5Ac (S)			potential sulphate or phosphate
0 OAc	1 OAc						2 OAc			
1	0.16	Man4+P		4	2	0	0	0	0	1
2	0.45	FMan4+P		4	2	1	0	0	0	1
3	1.23	Man5+P		5	2	0	0	0	0	1
4	0.15	Man5+P		5	2	0	0	0	0	1
		FA2G2S2(Ac)2		5	4	1	1	0	1	0
5	0.70	Man5+P		5	2	0	0	0	0	1
		FMan5+P		5	2	1	0	0	0	1
6	0.47	FMan5+P		5	2	1	0	0	0	1
		FA2G2S2(Ac)1		5	4	1	1	1	0	0
7	1.67	Man6+P		6	2	0	0	0	0	1
8,9	1.16	FA2G2S1		5	4	1	0	0	0	0
		Man6+P		6	2	0	0	0	0	1
10,11	0.62	FMan6+P		6	2	1	0	0	0	1
		Man6+P		6	2	0	0	0	0	1

12	3.05	FA2G2S2		5	4	1	2	0	0	0
13	0.48	FA2G2S1S1(Ac)2		5	4	1	1	0	1	0
		FA3G3S2(Ac)1		6	5	1	1	1	0	0
		FA2G2S2		5	4	1	2	0	0	0
		FA3G3S3(Ac)2		6	5	1	3	0	1	0
14,15	0.46	FA2G2S2		5	4	1	2	0	0	0
16	0.94	FA3G3S1		6	5	1	1	0	0	0

17	0.54	FA3G3S1		6	5	1	1	0	0	0
		FA4G4S3(Ac)2		7	6	1	1	2	0	0
18	1.96	FA3G3S2		6	5	1	2	0	0	0
		A3G3S2(Ac)4		6	5	0	0	0	2	0
19	1.62	FA3G3S2		6	5	1	2	0	0	0
		A3G3S2(Ac)4		6	5	0	0	0	2	0
		FA4G4S3(Ac)2		7	6	1	1	2	0	0
		FA4G4S4(Ac)2		7	6	1	2	2	0	0

20	5.32	FA3G3S3		6	5	1	3	0	0	0
21	1.76	FA4G4S1 or FA3G3S1(LacNAc)1		7	6	1	1	0	0	0
		FA3G3S3		6	5	1	3	0	0	0
		FA4G4S4(Ac)2		7	6	1	2	2	0	0
		FA4G4S3Ac		7	6	1	2	1	0	0

22	6.19	FA4G4S2 or FA3G3S2(LacNAc)1		7	6	1	2	0	0	0
		FA4G4S4		7	6	1	3	1	0	0
23	11.24	FA4G4S3 or FA3G3S3(LacNAc)1		7	6	1	3	0	0	0
		FA4G4S4Ac		7	6	1	3	1	0	0
24	12.96	FA4G4S4		7	6	1	4	0	0	0
25,26	2.78	FA4G4S2(LacNAc)1		8	7	1	2	0	0	0
27	9.83	FA4G4S3(LacNAc)1		8	7	1	3	0	0	0

28	1.31	FA4G4S3(LacNAc)1		8	7	1	3	0	0	0
		FA4G4S3Ac2(LacNAc)1		8	7	1	1	2	0	0
29	13.67	FA4G4S4(LacNAc)1		7	6	1	4	0	0	0
30	1.76	FA4G4S2(LacNAc)2		7	6	1	2	0	0	0
31	5.50	FA4G4S3(LacNAc)2		9	8	1	3	0	0	0
32	8.26	FA4G4S4(LacNAc)2		9	8	1	4	0	0	0
33	1.33	FA4G4S3(LacNAc)3		10	9	1	3	0	0	0
34	1.72	FA4G4S4(LacNAc)3		10	9	1	4	0	0	0